TITLE PAGE

Brain Response of a Computational Head Model for Prescribed Skull Kinematics and Simulated Football Helmet Impact Boundary Conditions

Authorship: David A. Bruneau[1], Duane S. Cronin[1]

[1]Department of MME, University of Waterloo, 200 University Avenue West, Waterloo, Canada

Submitted to: Journal of the Mechanical Behavior of Biomedical Materials

Running Title: Head Model Comparing Impact Boundary Conditions

Corresponding Author: Dr. Duane Cronin

Department of Mechanical Engineering

University of Waterloo

200 University Ave. West

Waterloo, Ontario, Canada, N2L 3G1

duane.cronin@uwaterloo.ca

(519) 888-4567 x32682

GRAPHICAL ABSTRACT

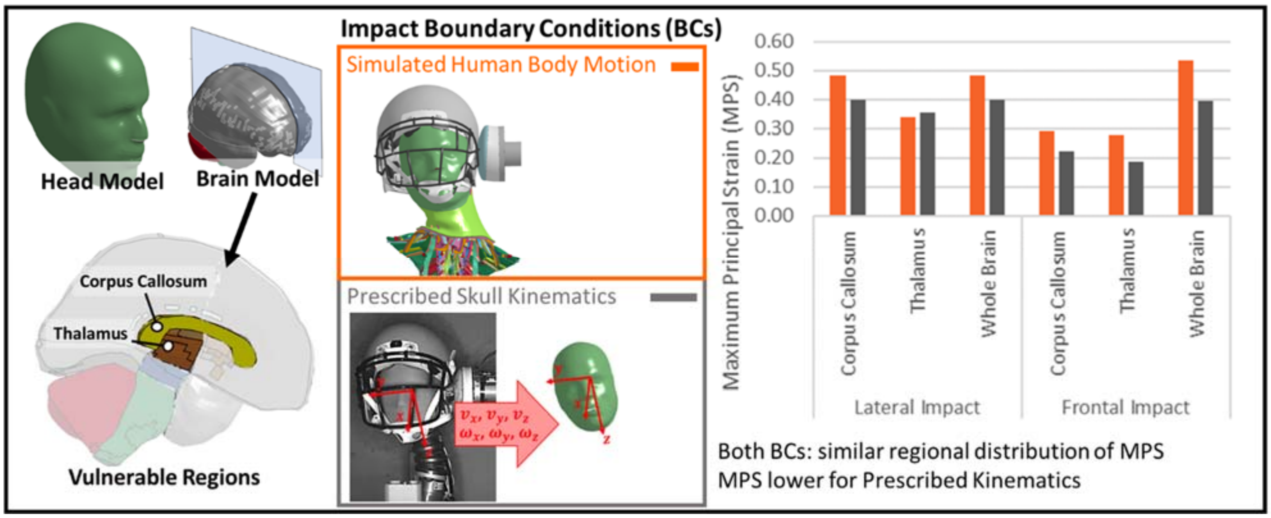

ABSTRACT

Computational human body models (HBM) present a novel approach to predict brain response in football impact scenarios, with prescribed kinematic boundary conditions for the HBM skull typically used at present. However, computational optimization of helmets requires simulation of the coupled helmet and HBM model; which is much more complex and has not been assessed in the context of brain deformation and existing simplified approaches. In the current study, two boundary conditions and the resulting brain deformations were compared using a HBM head model: (1) a prescribed skull kinematics (PK) boundary condition using measured head kinematics from experimental impacts; and (2) a novel detailed simulation of a HBM head and neck, helmet and linear impactor (HBM-S). While lateral and rear impacts exhibited similar levels of maximum principal strain (MPS) in the brain tissue using both boundary conditions, differences were noted in the frontal orientation (at 9.3 m/s, MPS was 0.39 for PK, 0.54 for HBM-S). Importantly, both PK and HBM-S boundary conditions produced a similar distribution of MPS throughout the brain for each impact orientation considered. Within the corpus callosum and thalamus, high MPS was associated with lateral impacts and lower values with frontal and rear impacts. The good correspondence of both boundary conditions is encouraging for future optimization of helmet designs. A limitation of the PK approach is the need for experimental head kinematics data, while the HBM-S can predict brain response for varying impact conditions and helmet configurations, with potential as a tool to improve helmet protection performance.

KEYWORDS

Helmet Protection, Human Body Model, Brain Deformation, Anthropometric Testing Device, Impact Biomechanics, Concussion, American Football

1. INTRODUCTION

Improvements to football helmets and mitigation of head injury can be informed by predicting head and brain responses in helmeted impacts, but require an accurate representation of the impact conditions. Specifically, finite element (FE) models of the human head can be used to estimate the deformation of the brain in football impact scenarios, based on measured or estimated head kinematics. The results of these simulations have been assessed using a variety of proposed brain deformation metrics, all of which have shown some degree of correlation with observed concussions (Beckwith et al., 2018; Hernandez et al., 2015; Kleiven, 2007; McAllister et al., 2012; Patton et al., 2015, 2013). While there is no consensus on which brain deformation metric is best for predicting concussion, one of the most commonly used metrics to quantify brain deformation is the maximum principal strain (MPS) of the brain tissue. This metric is thought to be predictive of injury severity (Hernandez et al., 2015; Jin et al., 2017; Kleiven, 2007; McAllister et al., 2012; Patton et al., 2015, 2013; Post et al., 2013; Viano et al., 2005) and therefore may be useful for evaluating helmet performance in a simulation environment. Furthermore, rotationally induced strains leading to stretching and disruption of axons is a theorized mechanism of concussion (Gennarelli, 2015; Ommaya and Gennarelli, 1974), which may be captured in part by MPS. When compared to MPS, another proposed brain deformation metric, the cumulative strain damage measure (CSDM), has not been as strongly related to concussion (Giordano and Kleiven, 2014; Hernandez et al., 2015; Kleiven, 2007; Patton et al., 2015). CSDM is defined as the percentage of brain tissue volume that exceeds a certain strain threshold. Previous studies have shown that brain deformation is induced primarily by angular motion (Beckwith et al., 2018; Kleiven, 2007) because the brain deforms primarily in shear. It is thought that brain deformation metrics may be better indicators of helmet performance than metrics solely based on the kinematics of the skull (Gabler et al., 2018), as the link between head kinematics and concussion is even less strong than the link between brain deformation and concussion (Hernandez et al., 2015). Consequently, evaluating helmets by computing brain deformation using HBM has been of increasing interest in the literature (Post et al., 2018, 2013).

A common method to determine the impact conditions relevant to head impact in football involves experimentally reconstructing helmeted impacts with an anthropometric testing device (ATD), and prescribing the measured head kinematics to a head FE model ("prescribed skull kinematics" (PK) boundary condition). The linear impactor experiment (Elkin et al., 2018; Post et al., 2013; Rousseau et al., 2010) is often used to re-create impact scenarios in a laboratory environment, which uses a coasting pneumatic ram to strike the head and neck of a Hybrid III ATD at a prescribed velocity. The ram is constrained to translate in one direction, and the ATD head and neck are mounted on a sliding table that can translate in the same direction as the ram. The measured head kinematics from the impact are then applied to the skull of a FE model of the human head (Figure 1~~Figure 1~~a). While this PK boundary condition is effective for investigating the performance of existing helmet designs or re-creating concussive impact events, investigating improvements to a helmet design requires building and testing a physical prototype to measure the required head kinematics, which can be costly and time consuming. The PK boundary condition is efficient for determining brain deformation in many impact orientations (Elkin et al., 2018). However, the biofidelity of the ATD neck is often cited as a limitation (Elkin et al., 2018) owing to the simplified structure and high stiffness relative to the human neck in some loading scenarios.

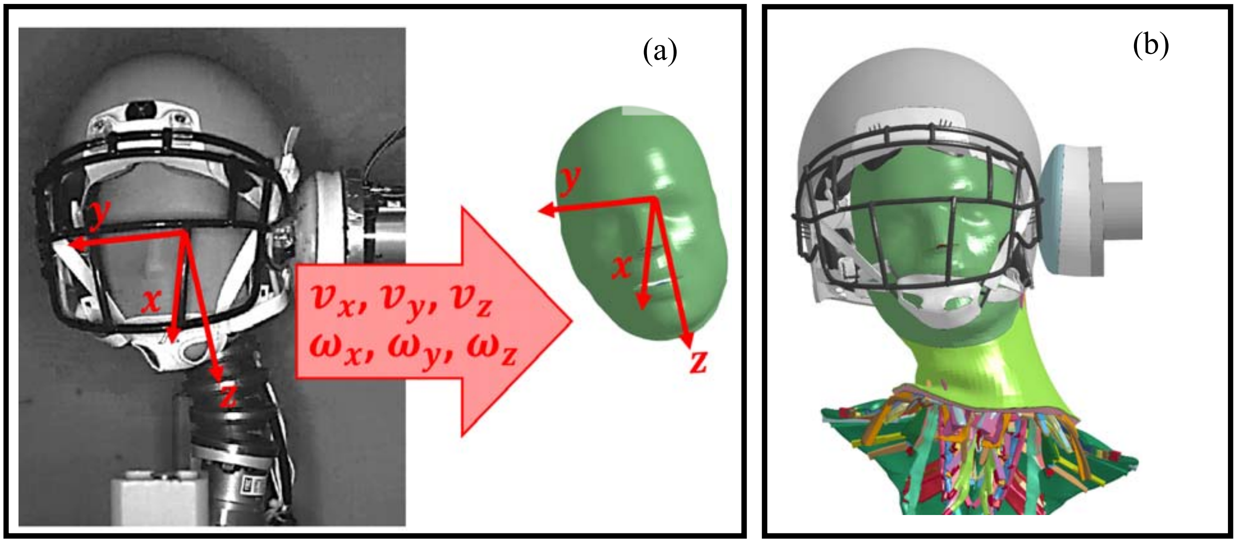

Figure 1 Lateral impact at 9.3 m/s, FE model with prescribed kinematics from experimental testing with Hybrid III head and neck (prescribed skull kinematics, PK) (a), and integrated HBM with helmet subjected to linear impact (simulated human body motion, HBM-S) (b)

A novel method to determine head kinematics is by reconstructing helmeted impacts computationally using a detailed human body model (HBM) coupled with a computational helmet model (Figure 1Figure 1b), which can provide additional anatomical detail compared to an ATD (Bruneau and Cronin, 2019). Furthermore, this simulated human body motion (HBM-S) boundary condition can be used as a testbed to make improvements to helmet design by allowing rapid iteration of helmet geometry and properties, and can be used to assess the interaction of effects that may be obscured by using a PK boundary condition. It has been shown that the head kinematics of the HBM are comparable to those of the ATD over short time frames (Bruneau and Cronin, 2019); however, it is possible that the neck could have an effect on brain response, which takes longer to reach maximum values relative to the kinematic responses (Sanchez et al., 2018). A common first step in assessing a HBM in a new impact scenario is by comparing responses to those of an ATD (Danelson et al., 2015; White et al., 2014). Previous studies have considered the head and neck (Bruneau and Cronin, 2019), or the full body impacts (Darling et al., 2016). These studies have predominantly used the Global Human Body Models Consortium (GHBMC) HBM (Bruneau and Cronin, 2019; Darling et al., 2016; Jin et al., 2017), a modern HBM with extensive experimental validation (Barker et al., 2017; Barker and Cronin, 2020) and a representation of passive and active neck muscle (Bruneau and Cronin, 2019).

When computing the brain response in a football helmet impact, it may be important to consider regional brain responses and multiple impact orientations. Some studies have suggested that the deep, inner regions of the brain are better predictors of concussion relative to other brain regions (Hernandez et al., 2015; Patton et al., 2015, 2013; Viano et al., 2005). Among these regions is the corpus callosum, which has been frequently found to be associated with concussion in the literature (Giordano and Kleiven, 2014; McAllister et al., 2012; Patton et al., 2015, 2013; Viano et al., 2005; Zhao et al., 2017), and the strain threshold for concussion in the corpus callosum is frequently found to be lower than the cerebrum white matter (Beckwith et al., 2018; Giordano and Kleiven, 2014; Kleiven, 2007; Patton et al., 2015). The thalamus (Giordano and Kleiven, 2014; Patton et al., 2015; Zhang et al., 2004) and midbrain (Giordano and Kleiven, 2014; Viano et al., 2005; Zhang et al., 2004) have also been associated with concussion. Another important factor in head impact is the impact orientation, with coronal plane rotation consistently leading to more brain injuries than sagittal plane rotation (Gennarelli et al., 1982; Lessley et al., 2018; Patton et al., 2013). The orientation sensitivity of concussion could be attributed to more sensitive brain regions, such as the corpus callosum, being affected more by coronal plane rotation than sagittal plane rotation (Hernandez et al., 2019). Surprisingly, previous HBM-S impact studies have not examined brain deformation in multiple impact planes (Darling et al., 2016; Jin et al., 2017).

Differing conclusions regarding the effect of neck muscle activation on head kinematics in football helmet impacts have been reported; from increasing head acceleration (Schmidt et al., 2014), to reducing head angular velocity and brain deformation (Jin et al., 2017), or showing no consistent effect on kinematics for varying head impact orientations (Bruneau and Cronin, 2019; Eckersley et al., 2020). Head kinematics at short durations (<40 ms post impact) have been shown to be mostly unaffected by active musculature (Bruneau and Cronin, 2019; Eckersley et al., 2020), but it is possible that the longer timeframe required for brain strains to develop results in active musculature having a larger effect on the brain response. The HBM-S boundary condition has not been widely evaluated in the literature to date, and has not been specifically compared to the PK boundary condition for predicted brain deformations.

The aim of the current study was to compare the brain response of a contemporary HBM using two impact boundary conditions: prescribed skull kinematics (PK) (Figure 1a) and simulated human body motion (HBM-S) (Figure 1Figure 1b) for six different impact cases. The PK boundary condition was applied using available experimental data, and a HBM was coupled with a detailed football helmet model (Corrales et al. 2019, Bustamante et al. 2019) and subjected to a linear impactor test condition for the HBM-S method. In addition, two neck muscle activation schemes were investigated for the HBM-S, representing a maximally and minimally tensed neck. The brain response was assessed using maximum principal strain (MPS, 95th Percentile) and cumulative strain damage measure (CSDM), for the whole brain, then in the corpus callosum, thalamus and midbrain, which have previously been linked to the risk of concussion (Hernandez et al., 2015; Patton et al., 2015, 2013; Viano et al., 2005).

2. MATERIAL AND METHODS

The GHBMC 50th percentile male head (Mao et al., 2013) and neck (Barker and Cronin, 2020) models were used in the current study. The measured head kinematics from linear impactor experiments with a contemporary football helmet (model: X2E 2016, size large, make: Xenith, LLC, Detroit, MI, USA) were applied to the isolated head model for the PK boundary condition, while the head and neck model was fitted with an FE model of the same Xenith X2e helmet as the experiment (Model Version 1.0, (Cronin et al., 2018)) and the integrated model was subjected to simulated linear impactor testing for the simulated human body motion (HBM-S) boundary condition. All models were solved using a commercial explicit FE code (LS-DYNA R7.1.2, LSTC, Livermore, California).

2.1. Impact Configurations

Six impact conditions (Lateral, Frontal and Rear, at 5.5 m/s and 9.3 m/s impact velocity) were investigated in the current study (Figure 2~~Figure 2~~), which were considered because head motions remained mostly in the coronal plane (lateral) or sagittal plane (frontal, rear), to induce distinctly different patterns of brain deformation (Meaney and Smith, 2012). The configuration of each impact orientation has been described previously (Giudice et al., 2018). An interval of 60 ms after initial contact with the impactor (t = 0) was analyzed for all impact scenarios, to allow the brain deformation metrics to fully develop over the course of the impact (Sanchez et al., 2018). This choice of interval also ensured that no secondary impacts between the helmet and fixture occurred.

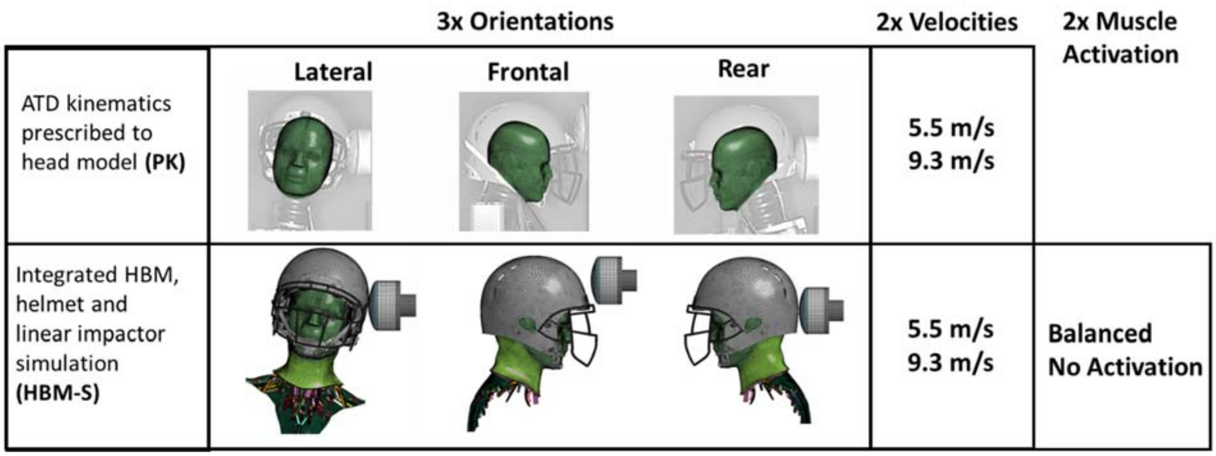

Figure 2 Matrix of simulation cases, showing six prescribed skull kinematics (PK) and twelve simulated human body motion (HBM-S) impact configurations. Three impact orientations were examined at two impact speeds for both conditions. Two muscle activation schemes were used for each speed and impact orientation for the HBM-S simulations.

2.2. Head and Brain Model

The brain model comprised 8 regions (Figure 3~~Figure 3~~). In addition to calculating whole brain values for strain metrics, 3 brain regions that have been most often correlated with observed concussion were considered in the current study (corpus callosum, thalamus, midbrain). The brain model used a Kelvin-Maxwell viscoelastic model for the brain tissue, with different stiffness for the white matter, grey matter and brainstem (Mao et al., 2013).

Maximum principal strain (MPS) was calculated from the brain model for each impact scenario, using logarithmic strain. The 95th percentile MPS has been proposed as an alternative to the 100th percentile principal strain (Elkin et al., 2018; Gabler et al., 2018; Panzer et al., 2012), to prevent a single element within the brain model from dominating the response. Additionally, it has been shown that 95th percentile MPS provides improved correlation with kinematic injury metrics compared to the 100th percentile value (Gabler et al., 2016), although both measures result in similar trends. The 95th percentile strain of each brain region was calculated separately, and the 95th percentile strain of the whole brain was calculated for all regions. Cumulative strain damage measure (CSDM), which is a measure of the proportion of elements that have exceed a certain threshold of MPS over the course of the impact, varying from 0.0 (no elements) to 1.0 (all elements) was calculated for each impact scenario. A threshold of 0.15 was used, which has been shown to be a good predictor of concussion (Sanchez et al., 2018) and diffuse axonal injury (Takhounts et al., 2003). In addition to the whole brain, CSDM was calculated for the corpus callosum, the thalamus and the midbrain regions. The time history of both MPS and CSDM were reported, similar to some previous FE studies of the brain (Darling et al., 2016; Kleiven, 2007), to highlight differences between the methodologies that may be obscured by simply reporting peak values.

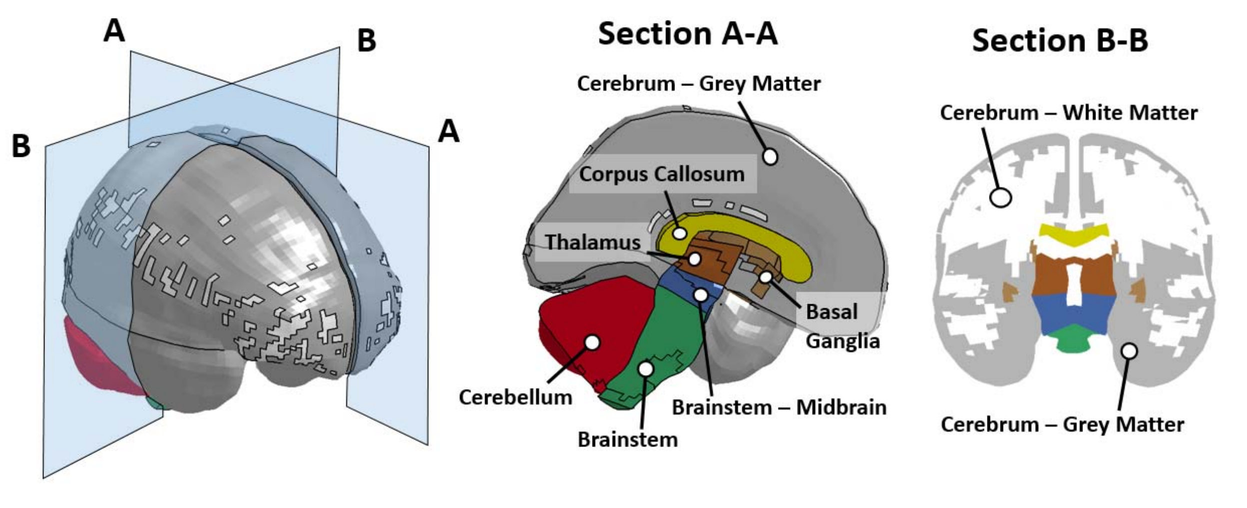

Figure 3 Brain regions in the HBM head. MPS and CSDM were considered for the whole brain, and for the corpus callosum, thalamus and midbrain regions.

2.3. Prescribed Skull Kinematics (PK) Boundary Condition

A series of experimental linear impactor tests were previously performed on a helmeted Hybrid III head and neck ATD following the NFL linear impactor test protocol (Funk et al., 2017), using the same modern football helmet (Xenith X2e) (Corrales et al., 2019) as the HBM-S impacts. A single experimental trial was conducted for each configuration, due to the low variability in these experiments (Pellman et al., 2006). The time histories of the angular and linear head velocity measured from the experiments were filtered with a CFC 180 filter (Newman et al., 2005) and applied to the isolated GHBMC head model. The skull of the head model was treated as rigid within the model in order to prescribe rigid-body kinematics to the head center of gravity, as has been done in previous studies (Sanchez et al., 2018; Zhang et al., 2004).

2.4. Simulated Human Body Motion (HBM-S) Boundary Condition

The GHBMC HBM has been previously verified and validated at the cervical spine level (Barker et al., 2017) and the full neck level (Barker and Cronin, 2020; Fice et al., 2011; Panzer et al., 2011). For the current study, vertebral fracture and skull fracture were disabled in the HBM. The boundary conditions for the HBM simulation matched those of the ATD experiment (Bruneau and Cronin, 2019), with translation of the first thoracic vertebrae (T1) only allowed in the global X direction, and mass added to T1 matching the mass of the carriage in the ATD experiment. In addition, the impactor mass and constraints used in the HBM simulations matched those of the ATD experiment (Funk et al., 2017). The impactor model consisted of an elastic end cap, a hyperelastic, viscoelastic foam material and a rigid backing plate and was validated at the material and subassembly level prior to validation in 8 bare-head linear impactor experiments (Giudice et al., 2018). The impactor was positioned with the same offsets relative to the head center of gravity as in the linear impactor experiments (Bruneau and Cronin, 2019). After coasting for the first 30 ms after the initial contact with the helmet, the impactor braking system was simulated by prescribing the impactor deceleration from the experiment. The head kinematics (velocity and acceleration, both angular and linear) from the simulations were filtered using CFC 180, as was done for the experimental kinematics, and can be found in Supplemental Materials C-F.

The open-source 2016 Xenith X2e helmet FE model used for the HBM-S impacts (Cronin et al., 2018)previously achieved excellent correspondence with experiments at the sub-assembly (Bustamante et al., 2019) and full helmet (Corrales et al., 2019) level. Fitting the helmet model to the HBM head required two pre-simulations (Bruneau and Cronin, 2019). In the first pre-simulation, a scaled representation of the skin geometry of the HBM head and neck was centered inside the helmet and expanded to the actual size and position, while the helmet moved freely. A second pre-simulation was used to tighten the helmet straps and locate the helmet in the final position, which matched the measurements taken prior to the ATD experiment. No pre-stress or pre-strain was carried over from the pre-simulations to the main simulation, as the helmet material strains were small (e.g. always less than 0.1 for the comfort foam).

Two muscle activation schemes were investigated in the current study. The “No Activation” scheme included only the passive muscle properties in the neck. The “Balanced Activation” scheme used a constant level of activation for the flexor and extensor muscles, with a 0.145:1

ratio of extensor to flexor activation, so that the neck was tensed and the head was stationary at the time of impact. A maximum activation level of 0.87 was used for the flexor muscles, which represents a very high level of muscle activation within physical limits (Bruneau and Cronin, 2019). With both muscle activation schemes, the head angle (using the Frankfort plane of the HBM), the neck angle (fitting a regression line through the center of mass of the 7 vertebrae of the HBM neck) and the head COG position of the HBM were matched with the ATD experiment (Bruneau and Cronin, 2019). The muscles were activated 80 ms prior to impact, to allow the head to reach equilibrium prior to impact ($V_{res} < 0.05$ m/s, $\omega_{res} < 0.15$ rad/s).

3. RESULTS

The PK boundary condition was first compared to the HBM-S with no muscle activation, in Section 3.1, 3.2 and 3.3. Selected strain metrics are reported in the manuscript, while the complete time-histories for strain metrics and kinematics are given in Supplemental Materials A-F. All reported strains in the article text refer to 95th percentile MPS.

The deformation of the brain followed a similar pattern in the PK and HBM-S simulations, where deformation of the inner regions of the brain lagged behind the outer regions, inducing shear strain (Figure 4~~Figure 4~~). In all lateral impacts, the corpus callosum, thalamus, and midbrain rotated predominantly in the coronal plane while in the frontal and rear impacts, these brain regions rotated in the sagittal plane. The space between the hemispheres of the brain was visibly curved in the coronal plane view of the brain in the lateral impact and the corpus callosum was visibly sheared compared to the frontal impact (Figure 4~~Figure 4~~). The direction of this curvature reversed later in time, corresponding with the second peak of MPS (Figure 5~~Figure 5~~).

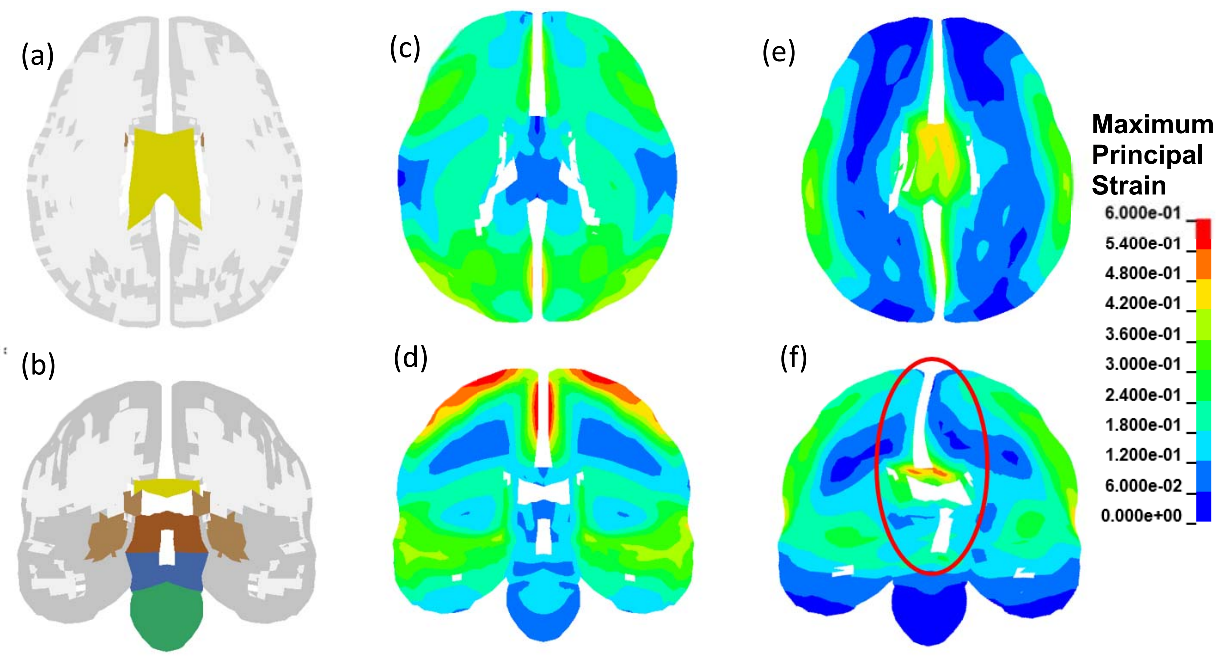

Figure 4 (a-b) Section planes through the brain model, following the same color scheme for brain regions as in Figure 3. (a) Transverse plane, (b) Coronal plane. (c-f) Peak maximum principal strain (MPS), simulated human body motion (HBM-S) impact at 9.3 m/s with no muscle activation. (c) Frontal impact, transverse plane, (d) Frontal impact, coronal plane (e) Lateral impact, axial plane, (f) Lateral impact, coronal plane. The coronal slices passed through the regions of maximum strain in both the frontal and lateral impact. The axial slice passed through the region of maximum strain in the lateral impact.

3.1. Whole Brain Response Metrics

The time response of MPS had two distinct peaks (Figure 5~~Figure 5~~) for both the PK and HBM-S simulations, where the first peak corresponded to a maximum shear deformation and the second peak represented a similar deformation in the reverse direction. The first peak occurred between 15 and 32 ms, and the second peak occurred between 40 and 60 ms. In the lateral impacts, the time between peaks was typically shorter compared to the frontal and rear (sagittal plane) impacts.

While the location and timing of peak 95th percentile MPS were similar with HBM-S and the PK boundary conditions (Table 1~~Table 1~~), the HBM-S exhibited predominantly higher values of whole brain MPS (from 0.25 to 0.54) relative to the PK boundary condition (from 0.20 to 0.40). Differences in MPS were largest (up to 0.14) in the frontal impact, where higher values of head angular velocity were observed (Table 1~~Table 1~~). No clear dependence on impact orientation was observed in whole brain MPS when comparing sagittal plane (frontal and rear) to coronal plane (lateral) impacts. In terms of timing, the maximum value of MPS typically occurred before the maximum angular velocity (Table 1~~Table 1~~ and Table 2~~Table 2~~). In most simulations, the first peak of MPS was the highest value of MPS, however in a few cases the second peak was higher (e.g. HBM-S frontal 5.5 m/s, PK rear 9.3 m/s).

(a)

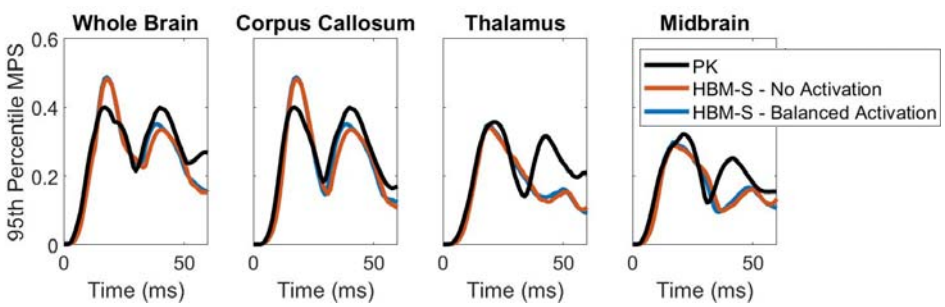

(b)

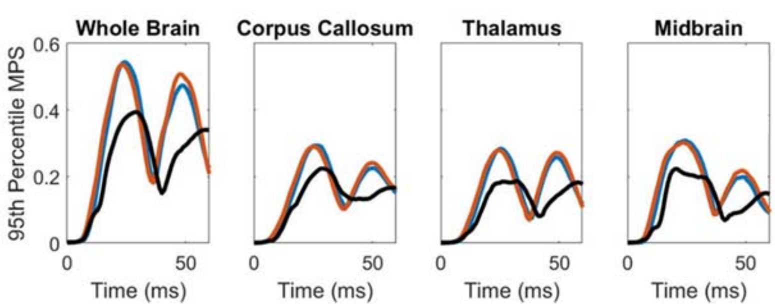

(c)

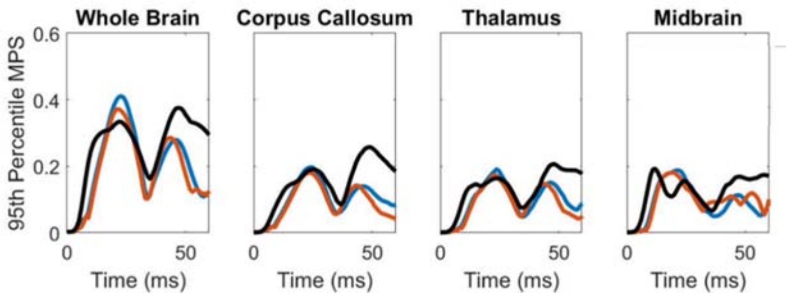

Figure 5 9.3 m/s impact, 95th Percentile Maximum Principal Strain in the (a) lateral, (b) frontal, and (c) rear impact directions.

Orientation	Speed	95th Percentile MPS PK	95th Percentile MPS HBM-S, No Activation	95th Percentile MPS HBM-S, Balanced Activation	95th Percentile MPS – Time of Maximum Value (ms) PK	95th Percentile MPS – Time of Maximum Value (ms) HBM-S, No Activation	95th Percentile MPS – Time of Maximum Value (ms) HBM-S, Balanced Activation
Lateral	5.5 m/s	0.33	0.33	0.28	21	22	18
	9.3 m/s	0.49	0.48	0.40	18	18	17
Frontal	5.5 m/s	0.34	0.32	0.22	54	53	32
	9.3 m/s	0.54	0.54	0.39	24	23	29
Rear	5.5 m/s	0.26	0.25	0.20	22	23	18
	9.3 m/s	0.41	0.37	0.38	23	21	47

Table 1 95th Percentile MPS peak values and timing for the whole brain. Peak values are color-coded with a gradient color scheme, ~~Peak values are color-coded,~~ **with darker red** cells ~~values~~ **indicating high peaks and** ~~white~~ lighter red cells ~~values~~ **indicating lower peaks.** ~~Dark green~~For the time of maximum value a binary color scheme is used, with ~~values indicate maximum in the first peak, yellow~~ blue cells **indicating**~~es~~ a **maximum in the second peak** and white cells indicating a maximum in the first peak**.**

CSDM followed similar trends to MPS for both the PK and HBM-S impact simulations. However, the CSDM results varied more between boundary conditions than MPS, with CSDM differences between the PK and HBM-S ranging from -0.15 to +0.27 (**Error! Reference source not found.**Table 3~~Table 3~~). The greatest difference was observed in the frontal orientation at 5.5 m/s. Interestingly, CSDM often increased in a stepwise manner after approximately 30 ms of simulation time (**Error! Reference source not found.**~~Table 2~~). The increases in whole brain CSDM after 30 ms were generally not large, with only three out of 18 simulations exhibiting a CSDM change greater than 0.10.

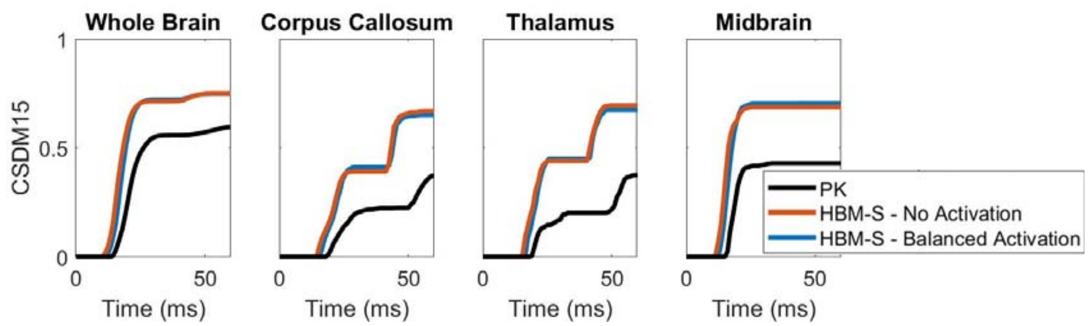

Figure 6 9.3 m/s impact, Cumulative Strain Damage Measure with a strain threshold of 0.15 (CSDM15) in the frontal orientation.

		Resultant Peak Angular Velocity (m/s)			Resultant Angular Velocity - Time of Peak Value (ms)		
Orientation	Speed	PK	HBM-S, No Activation	HBM-S, Balanced Activation	PK	HBM-S, No Activation	HBM-S, Balanced Activation
Lateral	5.5 m/s	29.7	32.5	29.9	25	26	23
	9.3 m/s	48.8	46.1	44.6	21	26	24
Frontal	5.5 m/s	22.0	31.3	34.4	50	30	30
	9.3 m/s	41.5	52.6	54.5	31	26	27
Rear	5.5 m/s	23.5	23.3	25.4	38	24	25
	9.3 m/s	40.6	37.9	40.1	24	53	23

Table 2 Angular velocity peak values and timing. Peak values and timing **are color-coded** with a gradient color scheme**, with darker red** cells ~~values~~ **indicating higher peaks and** ~~white~~ lighter red cells ~~values~~ **indicating lower peaks.** For the time of peak value, ~~Dark green values indicate maximum in the first peak, yellow~~ darker blue cells indicate ~~indicates maximum in the second peak~~a later peak value and lighter blue cells indicate an earlier peak value.~~,~~

		CSDM15			Increase in CSDM15 after 30ms		
Orientation	Speed	PK	HBM-S, No Activation	HBM-S, Balanced Activation	PK	HBM-S, No Activation	HBM-S, Balanced Activation
Lateral	5.5 m/s	0.13	0.17	0.18	0.03	0.02	0.02
	9.3 m/s	0.60	0.46	0.47	0.12	0.03	0.02
Frontal	5.5 m/s	0.14	0.41	0.48	0.05	0.14	0.13
	9.3 m/s	0.59	0.75	0.75	0.05	0.04	0.03
Rear	5.5 m/s	0.09	0.19	0.23	0.01	0.00	0.01
	9.3 m/s	0.58	0.52	0.58	0.10	0.02	0.01

Table 3 CSDM15 peak values for the whole brain (measured at 60ms), and the increase in CSDM that occurs between 30ms and 60ms of simulation time. Peak values are color-coded with a gradient color scheme**, with darker red** ~~values~~ cells **indicating higher** values ~~peaks~~ **and** ~~white~~ lighter red ~~values~~ cells **indicating lower**

~~peaks~~values. **For the increase after 30 ms, darker blue cells indicate a larger increase and lighter blue cells indicate a smaller increase.**

3.2. Regional Brain Response Metrics

The PK and HBM-S simulations had a similar distribution of strain throughout the brain in each impact orientation (Figure 7~~Figure 7~~). In the sagittal plane impacts (frontal and rear), MPS was consistently lower in the corpus callosum, thalamus and midbrain when compared to the lateral impact. In the lateral impacts of the HBM-S at 9.3 m/s, the peak MPS in the corpus callosum was always equal to the whole brain MPS, while the MPS in the thalamus and midbrain were 0.14 (29%) and 0.19 (40%) lower than the whole brain MPS respectively (Figure 7~~Figure 7~~). In the PK simulations, the MPS in the corpus callosum was equal to the full brain MPS as well, while the MPS in the thalamus was 0.04 (11%) lower than the whole brain MPS and the MPS in the midbrain was 0.08 (20%) lower than the full brain MPS. Further, in the frontal and rear impacts, the MPS in the inner brain regions was 0.19 to 0.26 (44 – 53%) lower than the whole brain MPS for the HBM-S impact, and 0.12 to 0.21 (31 – 53%) lower for the PK boundary condition. Despite the higher variability of CSDM, all lateral impacts had consistently higher values of CSDM in the inner regions of the brain than frontal and rear impacts (Supplemental Materials B). Notably, CSDM in certain brain regions had larger increases (up to 0.2) than whole brain CSDM after 30 ms; for example in the corpus callosum and thalamus in the frontal impact at 9.3 m/s (Figure 6~~Figure 6~~), which has a large increase in CSDM after 40 ms.

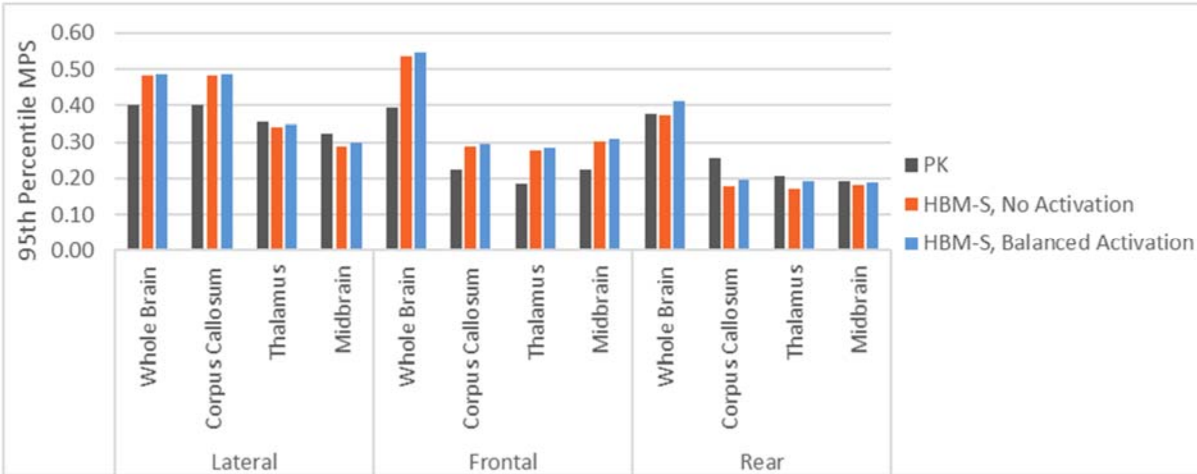

Figure 7   9.3 m/s impact, maximum value of 95th percentile MPS in each brain region across impact orientations

3.3. Effect of Balanced Muscle Activation

Within the HBM-S impacts, very small increases in peak whole brain MPS (up to 0.04) were observed with balanced muscle activation compared to the "no activation" condition (Table 1Table 1). The increase in MPS due to balanced muscle activation was smaller in the lateral orientation (increase of 0.01 in 9.3 m/s impact) compared to the frontal and rear orientations. Whole brain CSDM (Table 3Table 3) exhibited larger increases due to muscle activation than MPS, but these were still small with a maximum increase of 0.07 observed in CSDM. There was no notable change in the magnitude or timing of angular acceleration with muscle activation (Table 3).

4. DISCUSSION

4.1. Comparison of Prescribed Skull Kinematics (PK) and Simulated Human Body Motion (HBM-S) Whole-Brain Response

Overall, the HBM-S simulations predicted a similarly shaped MPS response curve to the PK boundary condition, with both simulation conditions exhibiting a bimodal response. However, the PK boundary condition generally predicted lower peak values of whole brain MPS than the HBM-S. The largest differences in whole brain MPS were observed in the frontal orientation (PK boundary condition predicted 0.09 to 0.14 lower MPS), where the sagittal angular velocity exhibited larger differences with the two boundary conditions. Smaller differences were observed in the lateral and rear orientations. In general, the peak angular velocity and acceleration were lower for the PK boundary condition (Table 2~~Table 3~~, Supplementary Materials C-D). The general trend of higher angular velocity magnitude for the HBM-S simulations was attributed to the longer neck of the HBM, and that the simulated helmet and impactor, while achieving excellent kinematic correlation with 60 experiments (Corrales et al., 2019) generally predicted slightly higher peak head kinematics than the experiment. As for the larger discrepancy in the frontal orientation, it has been previously shown that the head motion in this impact orientation can be influenced by the contact surface with the impactor (Giudice et al., 2018), which can be sensitive to small changes due to stick-slip between the impactor and facemask (Bruneau and Cronin, 2019), while the other two orientations had contact only between the smooth helmet shell and impactor cap. Accordingly, frontal linear impacts occurring predominantly in the sagittal plane have been shown to result in more widely varying angular kinematic responses than other orientations, with reported variations up to a factor of 3 in head angular acceleration observed between different helmets (Post et al., 2018). The good correspondence of MPS with both boundary conditions suggests that HBM-S impacts could be used to evaluate changes in MPS resulting from design changes to helmets.

Although injury thresholds have been proposed for computational brain models, the actual threshold values vary between different brain models (Ji et al., 2014; Post et al., 2013). The purpose of the current study was not to quantify the risk of concussion for the two boundary conditions considered, but to compare the variation in strain response when considering two boundary conditions for the same head model. The strain levels in the current study can be compared to the 95th percentile MPS computed for the NFL concussion reconstructions with the GHBMC head model (Sanchez et al., 2018), which found that the median 50% of NFL concussions had whole brain 95th percentile MPS between 0.3 and 0.43 (with a total range of 0.11 to 0.69). In the current study, MPS for the 9.3 m/s impacts, which is the mean impact speed for NFL concussions (Pellman et al., 2003), ranged from 0.38 to 0.40 for the PK boundary condition and from 0.37 to 0.54 for the HBM-S. The whole brain 95th percentile MPS was, on average, 0.07 higher for the HBM-S impact than with the PK boundary condition, which did not constitute a large change in injury metric considering the range of MPS in the NFL concussion reconstructions. Other studies have found an even greater range of variability in strain metrics for concussion and non-concussion outcomes (Beckwith et al., 2018; Hernandez et al., 2015). However, if using the HBM-S impact to optimize a helmet design, the systematically higher MPS for the HBM-S impact could result in a slightly different design outcome from what would be optimal for the PK boundary condition. However, it is perhaps more important that both simulation methods exhibited a similar regional distribution of strain throughout the brain in each impact orientation, and similar relative magnitudes comparing impact orientations for both boundary conditions.

The current study found that the maximum value of MPS often, but not always, occurred before 40 ms for both simulation conditions. The MPS of the whole brain exhibited a response with two peaks, with each peak corresponding with oscillatory shear deformation of the brain in opposite directions. The shear deformation of the brain is known to be caused primarily by rotational kinematics (Beckwith et al., 2018; Kleiven, 2007), because the initial rotation of the inner regions of the brain tends to lag the outside of the brain, corresponding with the first strain peak. The second peak corresponds a reversal of the brain deformation, due to the pre-stretch at the first peak (Figure 8~~Figure 8~~), and in various cases the second strain peak was either increased or reduced by the continued input kinematics to the head.

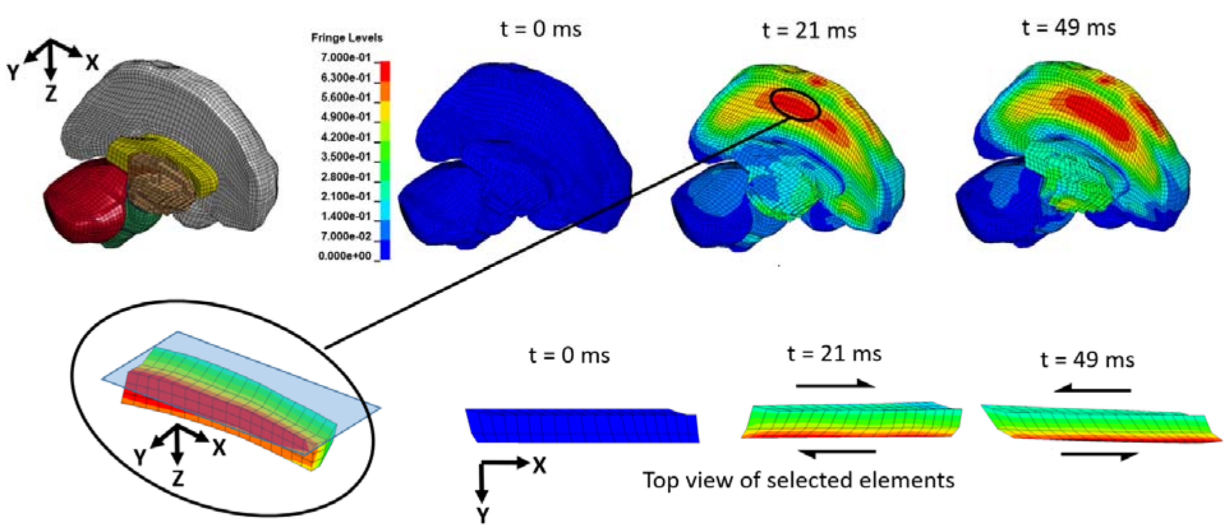

Figure 8 Progression of MPS in a frontal helmeted impact of the HBM (HBM-S, no activation) at 9.3 m/s. The visible shearing of the cerebrum grey and white matter elements in the center of the cranial fissure is highlighted.

Though the first peak corresponded to the maximum value of MPS in most impact cases, the second peak later in time was higher in some cases for the rear and frontal impacts, demonstrated by the much later timing of the maximum value of MPS (Table 1~~Table 1~~). The authors offer a potential explanation for this phenomenon with vibration theory (Laksari et al., 2018). The brain, like all structures, has resonant, or natural frequencies, and if an external oscillatory force has a similar frequency to one of the natural frequencies, the amplitude of brain deformation will increase. In the cases with a higher second MPS peak, the angular acceleration of the head resembles a sinusoid with a similar frequency to the resonant frequency of the brain, for example in the frontal impact of the HBM-S at 5.5 m/s (Figure 9~~Figure 9~~a). A previous study (Laksari et al., 2018) found that the natural frequency of the KTH brain model was approximately 20 Hz in the sagittal plane, or had a natural period of 50 ms. The GHBMC brain model in the current study had a similar natural period when estimated graphically; in the frontal HBM-S at 5.5 m/s, the strain peaks were 24 ms apart with balanced activation and 28 ms apart with no muscle activation (Figure 9~~Figure 9~~a). The natural period for MPS was therefore estimated as twice the distance between the strain peaks, and thus the natural frequency was in the range of 18 to 21 Hz. For the PK boundary condition (5.5 m/s, frontal impact), two distinct angular acceleration peaks were not observed (Figure 9~~Figure 9~~b), and therefore did not produce a high second peak in MPS. In this case, the angular acceleration had two peaks in the same direction approximately 30 ms apart, and thus partially offset the brain deformation caused by the initial impulse. This result implies that impact cases with a reversal in angular acceleration shortly after the initial impulse could exhibit higher MPS later in time, following the initial impact. Situations in football where there are two head impacts in quick succession may contribute to increased strains coinciding with the second peak if the head angular acceleration is close to the natural frequency of the brain, and therefore the frequency content of the head angular kinematics may be an overlooked contributor to concussions (Wu et al., 2018).

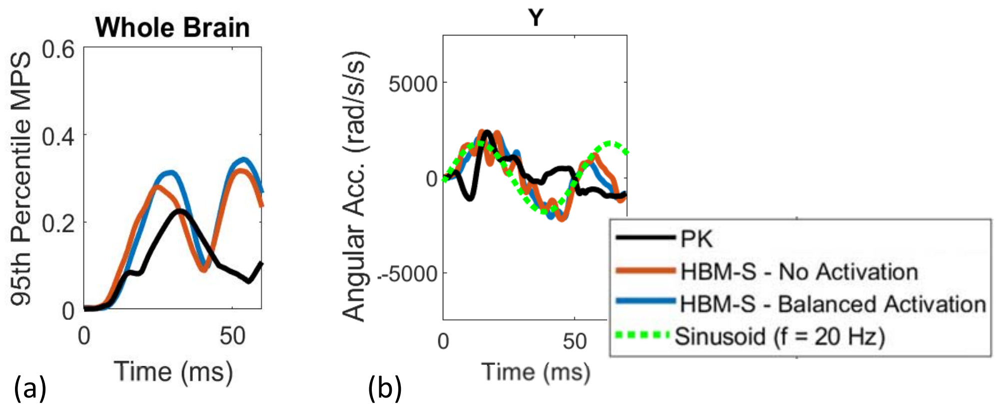

Figure 9 5.5 m/s frontal impact: whole brain MPS (a), and Y-angular acceleration with overlaid sinusoid at 20 Hz (b). The HBM-S impacts exhibited a near-sinusoidal angular acceleration trace close to the theorized natural frequency of the brain, while the angular acceleration in the PK case did not have a near-sinusoidal angular acceleration trace.

CSDM always reached maximum values after 40 ms, despite many previous studies considering only a 30 – 40 ms interval after impact (Sanchez et al., 2018). While the increases in CSDM after 40 ms were often small, CSDM nearly doubled in some brain regions after 40 ms (Figure 6~~Figure 6~~). This, in addition to the occurrence of peak MPS after 40 ms in some simulations in the current study, reinforces the assertion made by Sanchez et al., that considering brain deformation after 40 ms is important when simulating the brain in using kinematics from impact reconstructions (Sanchez et al., 2018). The shorter interval used in previous studies is one potential contributor to the weaker correlation of CSDM with observed concussions, in addition to the known sensitivity of CSDM to the chosen strain threshold. The current study also suggests that CSDM is more sensitive than MPS to small differences in head kinematics. The sensitivity likely occurs when the strain throughout the brain is close to the threshold strain, where relatively small changes in the actual strain can cause large jumps in CSDM. Additionally, the higher sensitivity of smaller brain regions can be explained by the presence of fewer elements compared to the whole brain; strain is typically more uniform over a smaller region and for a single element, CSDM will be maximally sensitive, equal to either 0 or 1. In summary, CSDM scales less linearly than MPS, especially in smaller brain regions, and the observed high sensitivity to small differences in input kinematics has been a suspected contributor to the lower correlation of CSDM with concussion than MPS observed in previous studies (Giordano and Kleiven, 2014; Hernandez et al., 2015; Kleiven, 2007; Patton et al., 2015). CSDM is based on the hypothesis that diffuse axonal injury is associated with the cumulative volume of brain tissue experiencing tensile strains over a certain threshold (Takhounts et al., 2003). However, proposed thresholds for CSDM vary considerably and past methods that have linked kinematics to measured concussions, such as impact reconstructions (Pellman et al., 2003; Sanchez et al., 2018) and instrumentation of players (Beckwith et al., 2018) have inherent error in the measured kinematics. In the future, it is possible that a discontinuous, sensitive metric with a well-defined threshold and precise input kinematics may be an excellent predictor of concussion. However, such metrics do not currently exist and until reliable injury thresholds are introduced, it may be better to use a continuous metric such as MPS to evaluate injury severity from brain models, where the variations in input kinematics translate more predictably to the output strain metric.

4.2. Regional Brain Response Metrics

While the relative magnitudes of whole brain MPS were typically higher in the HBM-S impacts compared to the PK boundary condition, both boundary conditions predicted considerably higher strains in the sensitive inner brain regions in the lateral orientation, compared to the frontal and rear impact orientations where the strain was highest elsewhere in the brain. The strains in the inner regions of the brain, including the corpus callosum (Giordano and Kleiven, 2014; McAllister et al., 2012; Patton et al., 2015, 2013; Zhao et al., 2017), the thalamus (Patton et al., 2013; Zhang et al., 2004) and the midbrain (Giordano and Kleiven, 2014; Zhang et al., 2004) have been more commonly correlated with observed concussions than other brain regions. Furthermore, proposed strain thresholds for concussion in the corpus callosum and thalamus in the literature are 1.15 to 2 times lower than proposed values in the cerebrum (Beckwith et al., 2018; Giordano and Kleiven, 2014; Kleiven, 2007; Patton et al., 2015). Interestingly, in every lateral impact in the current study, the corpus callosum was the brain region with the highest MPS (Figure 7~~Figure 7~~). In contrast, in all the frontal and rear impacts MPS was considerably lower in the thalamus (0.17 to 0.26 lower in the 9.3 m/s impacts), corpus callosum (0.12 to 0.25 lower) and midbrain (0.17 to 0.23 lower) than for the whole brain (Figure 7~~Figure 7~~). The strains in the thalamus were consistently higher in the lateral impacts than in frontal and rear impacts using both boundary conditions. The finding that lateral impacts consistently resulted in higher strains in regions linked with concussion supports the consistent observations in the literature that coronal rotations are more likely to cause TBI than sagittal plane impacts (Gennarelli et al., 1982; Hernandez et al., 2015; Meaney and Smith, 2012; Patton et al., 2013). Additionally, the increased strains observed in the inner brain regions could be a key contributor to the disproportionate amount of concussions (over 50%) in the 2015-2016 NFL season that resulted from lateral impacts, compared to other impact orientations (Lessley et al., 2018). The current study found that the whole brain MPS was less sensitive to impact orientation than the MPS within inner brain regions that have been correlated with concussion. In future studies, to improve helmet designs, the computational helmet model could be modified to reduce strain in vulnerable regions of the HBM brain model, using different thresholds for MPS in different brain regions.

4.3. Influence of Muscle Activation

The influence of active musculature on MPS on all regions of the brain was smaller than the difference between the two boundary conditions (the increase in MPS due to active muscle was always less than 0.04, or 10%). In previous work by the authors, it was found that active musculature had a similarly small effect on head angular velocity in the HBM-S boundary condition, with slight increases in angular velocity in frontal and rear impacts (Bruneau and Cronin, 2019). This finding echoes the results of Rousseau et al., who found that doubling the neck stiffness of an ATD in the linear impactor test did not have a significant influence on the head kinematics and therefore the resulting strains in the brain (Rousseau et al., 2010). Eckersley et al. previously suggested that tensed musculature increases head angular acceleration (Eckersley et al., 2020), which has been correlated with increased MPS and concussion risk (Hernandez et al., 2015; Patton et al., 2013), but that study used lower levels of loading. A numerical study (Bruneau and Cronin, 2019) has suggested that the reaction moment provided by the neck is far too small to provide significant resistance to the large force and moment created by the impactor, which consistently exceeded the resisting moment by a factor of twenty. While prescribing the same level of muscle activation to every flexor muscle, and a different constant value to all extensor muscles was a limitation of the current study, it was clear that the overall effect of active musculature was small due to the very high value of muscle activation used.

4.4. Limitations of this Study

The simplified PK and HBM-S impact boundary conditions considered in this study have some shared limitations, and others which are unique to each boundary condition. Both boundary conditions consider a 50th percentile male, that may not be representative of a typical football player, and different player anthropometrics may lead to different head kinematics owing to varying geometry and mass. As HBMs advance, subject specific models could be used to evaluate different player anthropometrics and address this limitation. Overall, HBMs have greater anatomical detail compared to ATDs and more biofidelic responses (White et al., 2014), which suggests that they are better approximations of real-world impacts to living people. The HBM-S impact boundary condition developed in the current study could be particularly useful for evaluating the response of specific brain regions to helmet modifications, especially once more reliable links between specific brain regions and head injury metrics are established. In addition, HBM-S could be beneficial for evaluating brain response to off-axis impacts and impacts with considerable axial neck loading, which are typically avoided by testing protocols. The ATD neck has limited biofidelity in these impact orientations (Yoganandan et al., 1989), while the HBM-S neck has been validated in axial torsion and tension (Barker and Cronin, 2020). The Hybrid III neck has limited biofidelity in axial compression, though this is thought to have a larger effect on the axial linear acceleration of the head compared to the sagittal or coronal angular velocity (Bruneau and Cronin, 2019), which are the main contributors to brain deformation in the current study. While the PK boundary condition remains useful, as it can be used to evaluate existing helmets in a variety of impact conditions with relative ease, it is limited to impact scenarios for which experimental kinematics have been measured. Finally, the brain model used in the current study incorporated cadaveric material properties and was assessed using experimentally measured brain displacement data from post-mortem human surrogates (Mao et al., 2013), where the brain tissue is known to behave differently compared to *in vivo* tissue. Ongoing work on the GHBMC model aims to incorporate improved material properties and validation data as these become available.

4.5. Conclusions

The purpose of the current study was to compare the brain response in a football helmet impact scenario for a novel HBM simulation method (HBM-S) with an established method using prescribed skull kinematics (PK) measured from ATD impact experiments. Overall, the peak MPS for the HBM-S was higher than for the PK boundary condition, for a given impact orientation and speed. For example, in a 9.3 m/s frontal impact, the MPS was 0.54 in the HBM-S, and 0.39 with PK boundary condition. Importantly, both boundary conditions resulted in a similar regional distribution of MPS throughout the brain. The MPS in the inner regions of the brain, especially the corpus callosum, were consistently higher in all lateral impacts than in all rear and frontal impacts, for both boundary conditions. Within the HBM-S, small increases in MPS were observed in all impact orientations when the neck muscles were activated at their maximal contraction, but the effect of muscle activation was relatively small compared to the difference between boundary conditions.

The Cumulative Strain Damage Measure (CSDM) exhibited similar trends to MPS when comparing magnitude of CSDM with the two boundary conditions, and the regional distribution of CSDM, albeit with more variability. The CSDM metric responded non-linearly to changes in kinematics, was often sensitive to small changes in kinematics, and was more sensitive in smaller brain regions. These effects were attributed to the strain in the brain model being close to the chosen threshold. Occasionally, CSDM exhibited large increases at times between 40 ms to 60 ms after impact, a timeframe not often considered in previous studies.

Overall, the good correspondence of MPS response for both the PK and HBM-S boundary conditions suggests that the HBM-S boundary condition developed in the current study is a viable tool to investigate and optimize head protection in future studies.

ACKNOWLEDGMENTS

The authors would like to acknowledge the Global Human Body Models Consortium for use of the HBM, and Biocore LLC for the ATD experimental data, and the helmet and impactor model.

The research presented was made possible by a grant from Football Research, Inc. (FRI), the National Football League (NFL), and Biomechanical Consulting and Research, LLC (Biocore) in the USA. The authors acknowledge the contributions of the NFLPA. The views expressed are solely those of the authors and do not represent those of FRI, the NFL, Biocore, or any of their affiliates or funding sources.

REFERENCES

Barker, J.B., Cronin, D.S., 2020. Multilevel Validation of a Male Neck Finite Element Model With Active Musculature. J. Biomech. Eng. https://doi.org/10.1115/1.4047866

Barker, J.B., Cronin, D.S., Nightingale, R.W., 2017. Lower Cervical Spine Motion Segment Computational Model Validation: Kinematic and Kinetic Response for Quasi-Static and Dynamic Loading. J. Biomech. Eng. 139, 061009. https://doi.org/10.1115/1.4036464

Beckwith, J.G., Zhao, W., Ji, S., Ajamil, A.G., Bolander, R.P., Chu, J.J., McAllister, T.W., Crisco, J.J., Duma, S.M., Rowson, S., Broglio, S.P., Guskiewicz, K.M., Mihalik, J.P., Anderson, S., Schnebel, B., Gunnar Brolinson, P., Collins, M.W., Greenwald, R.M., 2018. Estimated Brain Tissue Response Following Impacts Associated With and Without Diagnosed Concussion. Ann. Biomed. Eng. 46, 819–830. https://doi.org/10.1007/s10439-018-1999-5

Bruneau, D.A., Cronin, D.S., 2019. Head and Neck Response of an Active Human Body Model and Finite Element Anthropometric Test Device During a Linear Impactor Helmet Test. J. Biomech. Eng. https://doi.org/10.1115/1.4043667

Bustamante, M., Bruneau, D., Barker, J., Gierczycka, D., Corrales, M., Cronin, D., 2019. Component-Level Finite Element Model and Validation for a Modern American Football Helmet. J. Dyn. Behav. Mater. https://doi.org/https://doi.org/10.1007/s40870-019-00189-9

Corrales, M.A., Gierczycka, D., Barker, J., Bruneau, D., Bustamante, M.C., Cronin, D.S., 2019. Validation of a Football Helmet Finite Element Model and Quantification of Impact Energy

Distribution. Ann. Biomed. Eng. 48, 121–132. https://doi.org/10.1007/s10439-019-02359-1

Cronin, D., Barker, J., Gierczycka, D., Bruneau, D., Bustamante, M., Corrales, M., 2018. User Manual - Finite Element Model of 2016 Xenith X2E (Safety Equipment Institute model X2E) Version 1.0 for LS-DYNA [WWW Document]. URL http://biocorellc.com/resources/

Danelson, K.A., Golman, A.J., Kemper, A.R., Scott Gayzik, F., Clay Gabler, H., Duma, S.M., Stitzel, J.D., 2015. Finite element comparison of human and Hybrid III responses in a frontal impact. Accid. Anal. Prev. 85, 125–156. https://doi.org/10.1016/j.aap.2015.09.010

Darling, T., Muthuswamy, J., Rajan, S.D., 2016. Finite element modeling of human brain response to football helmet impacts. Comput. Methods Biomech. Biomed. Engin. 19, 1432–1442. https://doi.org/10.1080/10255842.2016.1149574

Eckersley, C.P., Nightingale, R.W., Luck, J.F., Bass, C.R., 2020. The role of cervical muscles in mitigating concussion. J. Sci. Med. Sport 5–9. https://doi.org/10.1016/j.jsams.2019.01.009

Elkin, B.S., Gabler, L.F., Panzer, M.B., Siegmund, G.P., 2018. Brain tissue strains vary with head impact location: A possible explanation for increased concussion risk in struck versus striking football players. Clin. Biomech. 1–9. https://doi.org/10.1016/j.clinbiomech.2018.03.021

Fice, J.B., Cronin, D.S., Panzer, M.B., 2011. Cervical spine model to predict capsular ligament response in rear impact. Ann. Biomed. Eng. 39, 2152–2162. https://doi.org/10.1007/s10439-011-0315-4

Funk, J.R., Crandall, J., Wonnacott, M., Withnall, C., 2017. Linear Impactor Helmet Test Protocol.

Gabler, L.F., Crandall, J.R., Panzer, M.B., 2018. Development of a Metric for Predicting Brain Strain

Responses Using Head Kinematics. Ann. Biomed. Eng. 46, 972–985. https://doi.org/10.1007/s10439-018-2015-9

Gabler, L.F., Crandall, J.R., Panzer, M.B., 2016. Assessment of Kinematic Brain Injury Metrics for Predicting Strain Responses in Diverse Automotive Impact Conditions. Ann. Biomed. Eng. 44, 3705–3718. https://doi.org/10.1007/s10439-016-1697-0

Gennarelli, T.A., 2015. The Centripetal Theory of Concussion (CTC) revisited after 40 years and a proposed new Symptomcentric Concept of the Concussions, in: IRCOBI Conference 2015. pp. 1131–1138. https://doi.org/10.2353/ajpath.2009.080794

Gennarelli, T.A., Thibault, L.E., Adams, J.H., Graham, D.I., Thompson, C.J., Marcincin, R.P., 1982. Diffuse axonal injury and traumatic coma in the primate. Ann. Neurol. 12, 564–574. https://doi.org/10.1002/ana.410120611

Giordano, C., Kleiven, S., 2014. Evaluation of Axonal Strain as a Predictor for Mild Traumatic Brain Injuries Using Finite Element Modeling. Stapp Car Crash J. 58, 29–61.

Giudice, J.S., Park, G., Kong, K., Bailey, A., Kent, R., Panzer, M.B., 2018. Development of Open-Source Dummy and Impactor Models for the Assessment of American Football Helmet Finite Element Models. Ann. Biomed. Eng. 1–27.

Hernandez, F., Giordano, C., Goubran, M., Parivash, S., Grant, G., Zeineh, M., 2019. Lateral impacts correlate with falx cerebri displacement and corpus callosum trauma in sports - related concussions. Biomech. Model. Mechanobiol. https://doi.org/10.1007/s10237-018-01106-0

Hernandez, F., Wu, L.C., Yip, M.C., Laksari, K., Hoffman, A.R., Lopez, J.R., Grant, G.A., Kleiven, S., Camarillo, D.B., 2015. Six Degree-of-Freedom Measurements of Human Mild Traumatic Brain Injury. Ann. Biomed. Eng. 43, 1918–1934. https://doi.org/10.1007/s10439-014-1212-4

Ji, S., Ghadyani, H., Bolander, R.P., Beckwith, J.G., Ford, J.C., McAllister, T.W., Flashman, L.A., Paulsen, K.D., Ernstrom, K., Jain, S., Raman, R., Zhang, L., Greenwald, R.M., 2014. Parametric comparisons of intracranial mechanical responses from three validated finite element models of the human head. Ann. Biomed. Eng. 42, 11–24. https://doi.org/10.1007/s10439-013-0907-2

Jin, X., Feng, Z., Mika, V.H., Li, H., Viano, D., Yang, K.H., 2017. The Role of Neck Muscle Activities on the Risk of Mild Traumatic Brain Injury in American Football. J. Biomech. Eng. 139. https://doi.org/10.1115/1.4037399

Kleiven, S., 2007. Predictors for traumatic brain injuries evaluated through accident reconstructions. Stapp Car Crash J. 51, 81–114. https://doi.org/2007-22-0003 [pii]

Laksari, K., Kurt, M., Babaee, H., Kleiven, S., Camarillo, D., 2018. Mechanistic Insights into Human Brain Impact Dynamics through Modal Analysis. Phys. Rev. Lett. 120, 138101. https://doi.org/10.1103/PhysRevLett.120.138101

Lessley, D.J., Kent, R.W., Funk, J.R., Sherwood, C.P., Cormier, J.M., Crandall, J.R., Arbogast, K.B., Myers, B.S., 2018. Video Analysis of Reported Concussion Events in the National Football League During the 2015-2016 and 2016-2017 Seasons. Am. J. Sports Med. 46, 3502–3510. https://doi.org/10.1177/0363546518804498

Mao, H., Zhang, L., Jiang, B., Genthikatti, V. V., Jin, X., Zhu, F., Makwana, R., Gill, A., Jandir, G., Singh, A., Yang, K.H., 2013. Development of a Finite Element Human Head Model Partially Validated With Thirty Five Experimental Cases. J. Biomech. Eng. 135, 111002. https://doi.org/10.1115/1.4025101

McAllister, T.W., Ford, J.C., Ji, S., Beckwith, J.G., Flashman, L.A., Paulsen, K., Greenwald, R.M., 2012. Maximum principal strain and strain rate associated with concussion diagnosis correlates with changes in corpus callosum white matter indices. Ann. Biomed. Eng. 40, 127–140. https://doi.org/10.1007/s10439-011-0402-6

Meaney, D.F., Smith, D.H., 2012. Biomechanics of concussion. Clin. Sport. Med. 30, 14–27. https://doi.org/10.1159/000358748

Newman, J.A., Beusenberg, M.C., Shewchenko, N., Withnall, C., Fournier, E., 2005. Verification of biomechanical methods employed in a comprehensive study of mild traumatic brain injury and the effectiveness of American football helmets. J. Biomech. 38, 1469–1481. https://doi.org/10.1016/j.jbiomech.2004.06.025

Ommaya, A.K., Gennarelli, T.A., 1974. Cerebral Concussion and Traumatic Unconsciousness. Brain 97, 633–654. https://doi.org/10.1093/brain/97.1.633

Panzer, M.B., Fice, J.B., Cronin, D.S., 2011. Cervical spine response in frontal crash. Med. Eng. Phys. 33, 1147–1159. https://doi.org/10.1016/j.medengphy.2011.05.004

Panzer, M.B., Myers, B.S., Capehart, B.P., Bass, C.R., 2012. Development of a finite element model for blast brain injury and the effects of CSF cavitation. Ann. Biomed. Eng. 40, 1530–1544.

https://doi.org/10.1007/s10439-012-0519-2

Patton, D., McIntosh, A., Kleiven, S., 2015. The Biomechanical Determinants of Concussion: Finite Element Simulations to Investigate Tissue-Level Predictors of Injury During Sporting Impacts to the Unprotected Head. J. Appl. Biomech. 721–730. https://doi.org/10.1123/jab.2014-0223

Patton, D., McIntosh, A., Kleiven, S., 2013. The Biomechanical Determinants of Concussion: Finite Element Simulations to. J. Appl. Biomech. 721–730. https://doi.org/10.1123/jab.2014-0223

Pellman, E.J., Viano, D.C., Tucker, A.M., Casson, I.R., Waeckerle, J.F., Maroon, J.C., Lovell, M.R., Collins, M.W., Kelly, D.F., Valadka, A.B., Cantu, R.C., Bailes, J.E., Levy, M.L., 2003. Concussion in professional football: Reconstruction of game impacts and injuries. Neurosurgery 53, 799–814. https://doi.org/10.1093/neurosurgery/53.3.799

Pellman, E.J., Viano, D.C., Withnall, C., Shewchenko, N., Bir, C.A., Halstead, P.D., 2006. Concussion in professional football: Helmet testing to assess impact performance - Part 11. Neurosurgery 58, 78–95. https://doi.org/10.1227/01.NEU.0000196265.35238.7C

Post, A., Kendall, M., Cournoyer, J., Karton, C., Oeur, R.A., Dawson, L., Hoshizaki, T.B., Post, A., Kendall, M., Cournoyer, J., Karton, C., Oeur, R.A., 2018. Brain tissue analysis of impacts to American football helmets. Comput. Methods Biomech. Biomed. Engin. 5842, 1–14. https://doi.org/10.1080/10255842.2018.1445229

Post, A., Oeur, A., Hoshizaki, B., Gilchrist, M.D., 2013. An examination of American football helmets using brain deformation metrics associated with concussion. Mater. Des. 45, 653–

662. https://doi.org/10.1016/j.matdes.2012.09.017

Rousseau, P., Hoshizaki, T.B., Gilchrist, M.D., 2010. Title Estimating the influence of neckform compliance on brain tissue strain during a Helmeted impact.

Sanchez, E.J., Gabler, L.F., Good, A.B., Funk, J.R., Crandall, J.R., Panzer, M.B., 2018. A reanalysis of football impact reconstructions for head kinematics and finite element modeling. Clin. Biomech. https://doi.org/10.1016/j.clinbiomech.2018.02.019

Schmidt, J.D., Guskiewicz, K.M., Blackburn, J.T., Mihalik, J.P., Siegmund, G.P., Marshall, S.W., 2014. The influence of cervical muscle characteristics on head impact biomechanics in football. Am. J. Sports Med. 42, 2056–2066. https://doi.org/10.1177/0363546514536685

Takhounts, E.G., Eppinger, R.H., Campbell, J.Q., Tannous, R.E., Power, E.D., Shook, L.S., 2003. On the development of the SIMon finite element head model. Stapp Car Crash J 47, 107–33. https://doi.org/2003-22-0007 [pii]

Viano, D.C., Casson, I.R., Pellman, E.J., Zhang, L., King, A.I., Yang, K.H., 2005. Concussion in professional football: Brain responses by finite element analysis: Part 9. Neurosurgery 57, 891–915. https://doi.org/10.1227/01.NEU.0000186950.54075.3B

White, N.A., Danelson, K.A., Scott Gayzik, F., Stitzel, J.D., 2014. Head and Neck Response of a Finite Element Anthropomorphic Test Device and Human Body Model During a Simulated Rotary-Wing Aircraft Impact. J. Biomech. Eng. 136, 111001. https://doi.org/10.1115/1.4028133

Wu, L.C., Kuo, C., Loza, J., Kurt, M., Laksari, K., Yanez, L.Z., Senif, D., Anderson, S.C., Miller, L.E., Urban, J.E., Stitzel, J.D., Camarillo, D.B., 2018. Detection of American Football Head Impacts Using Biomechanical Features and Support Vector Machine Classification. Sci. Rep. 8, 1–14. https://doi.org/10.1038/s41598-017-17864-3

Yoganandan, N., A. Sances, J., Pintar, F., 1989. Biomechanical Evaluation of the Axial Compressive Responses of the Human Cadaveric and Manikin Necks. J Biomech Eng 111, 250–255.

Zhang, L., Yang, K.H., King, A.I., 2004. A Proposed Injury Threshold for Mild Traumatic Brain Injury. J. Biomech. Eng. 126, 226. https://doi.org/10.1115/1.1691446

Zhao, W., Cai, Y., Li, Z., Ji, S., 2017. Injury prediction and vulnerability assessment using strain and susceptibility measures of the deep white matter. Biomech. Model. Mechanobiol. 16, 1709–1727. https://doi.org/10.1007/s10237-017-0915-5

Supplemental Materials A: 95th Percentile MPS in all impacts

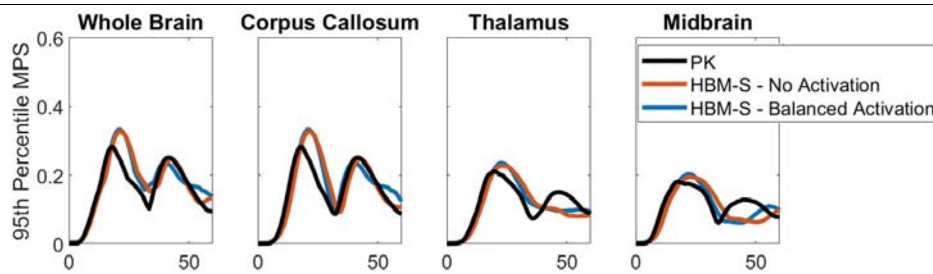

5.5 m/s

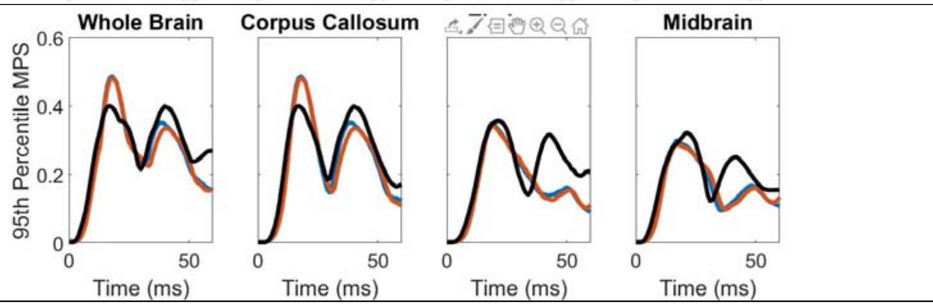

9.3 m/s

Lateral Orientation

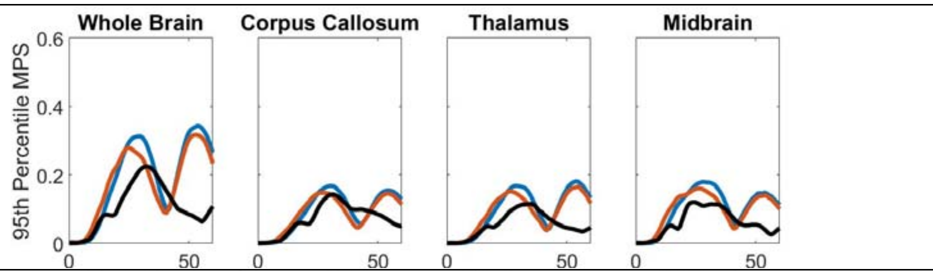

5.5 m/s

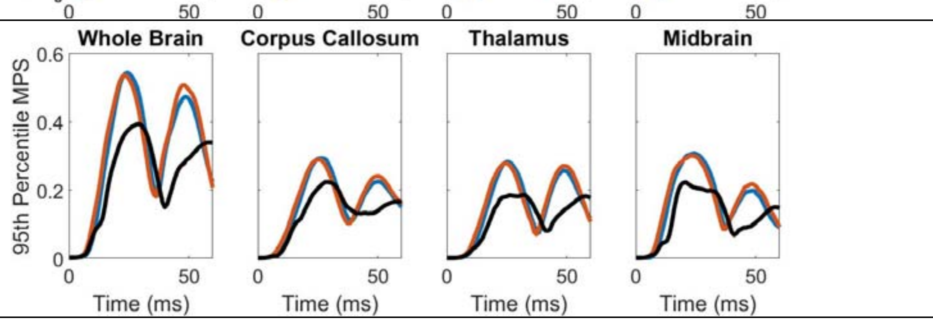

9.3 m/s

Frontal Orientation

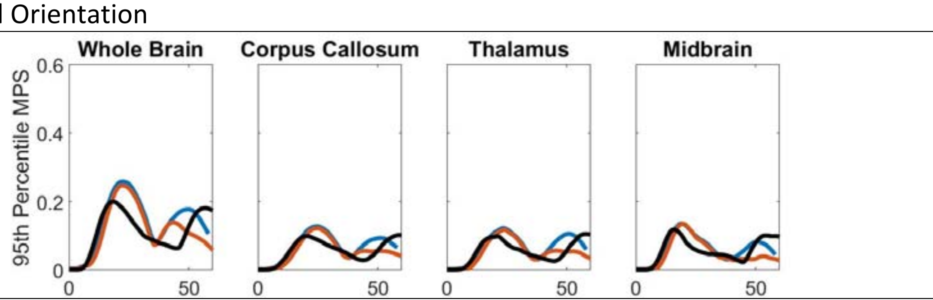

5.5 m/s

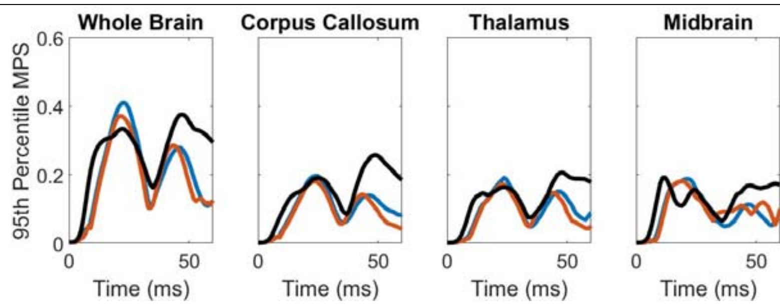 	9.3 m/s
Rear Orientation	

Figure S1 95th Percentile MPS in all impacts

Supplemental Materials B: CSDM in all impacts

<table>
<tr><td>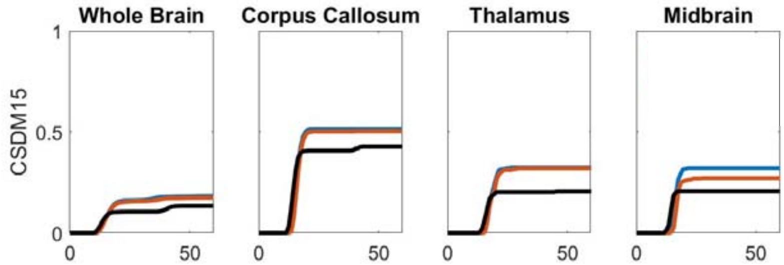
</td><td>5.5 m/s</td></tr>
<tr><td>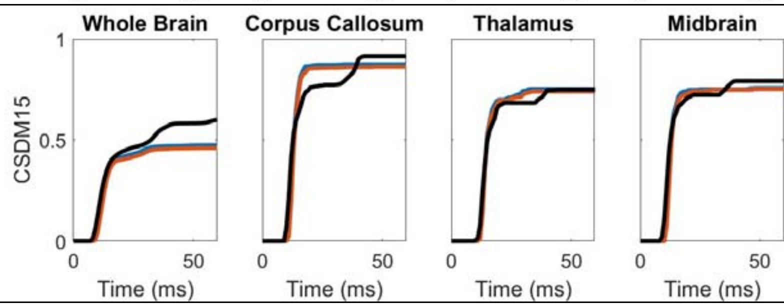
</td><td>9.3 m/s</td></tr>
<tr><td>Lateral Orientation</td><td></td></tr>
<tr><td>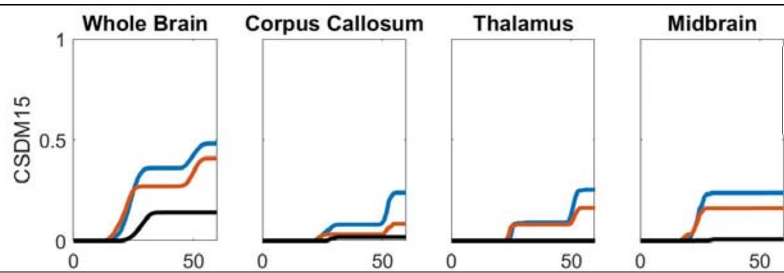
</td><td>5.5 m/s</td></tr>
<tr><td>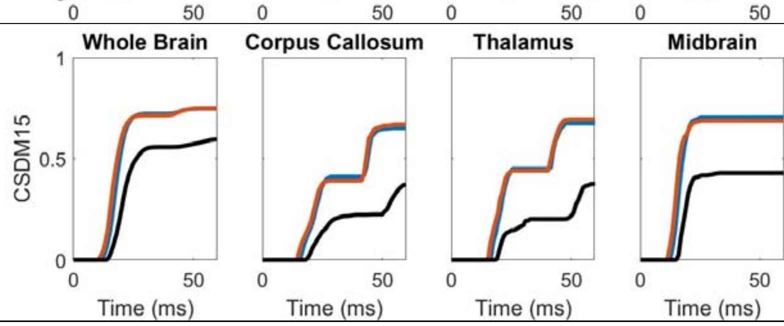
</td><td>9.3 m/s</td></tr>
<tr><td>Frontal Orientation</td><td></td></tr>
<tr><td>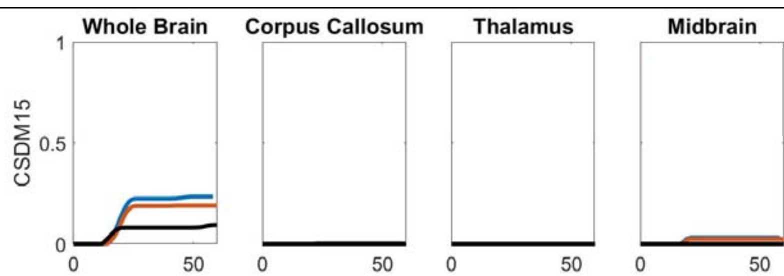
</td><td>5.5 m/s</td></tr>
</table>

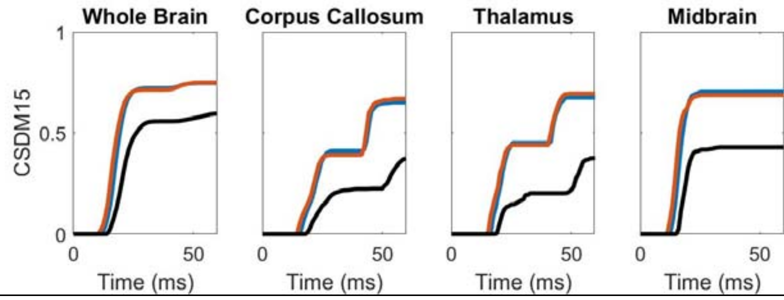	9.3 m/s
Rear Orientation	

Figure S2 CSDM in all impacts

Supplemental Materials C: Head Angular Velocity (3DOF) in all impacts

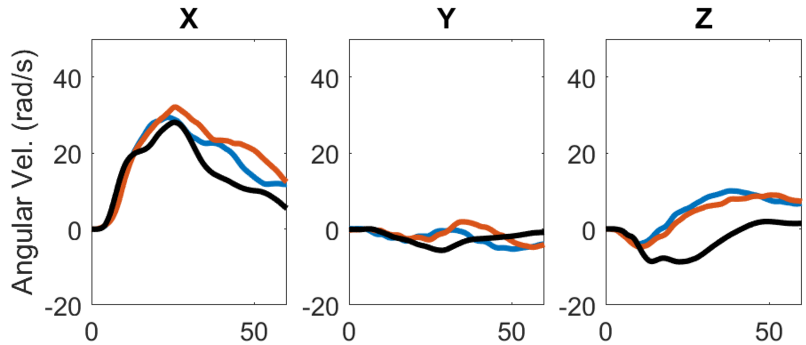

5.5 m/s

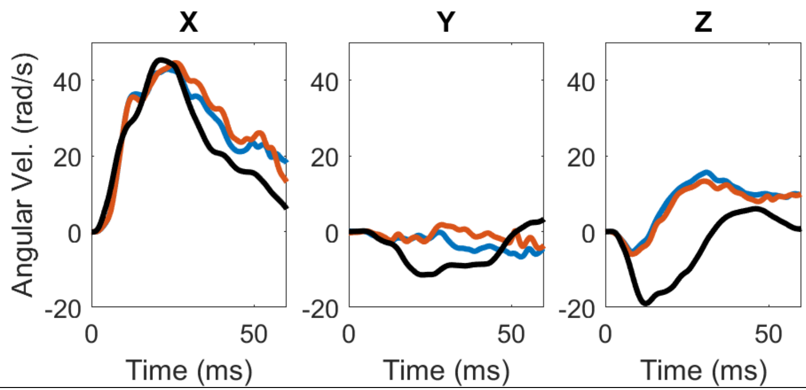

9.3 m/s

Lateral Orientation

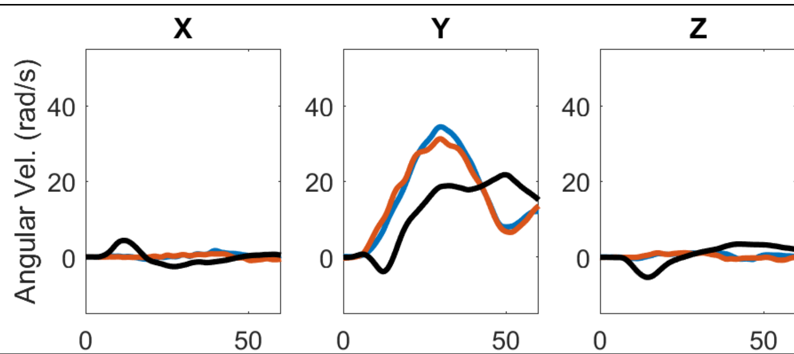

5.5 m/s

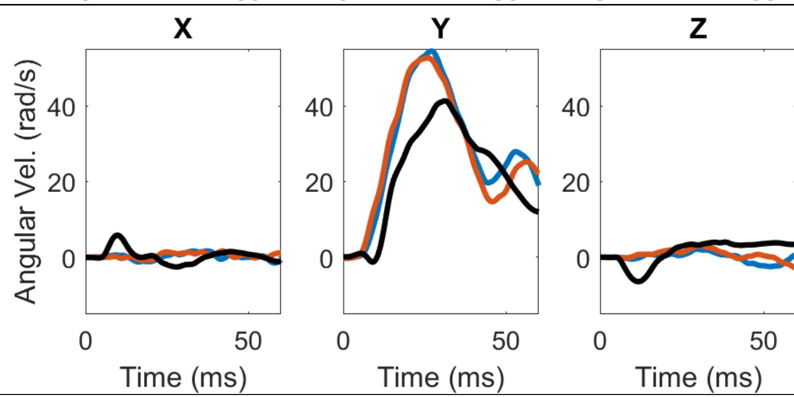

9.3 m/s

Frontal Orientation

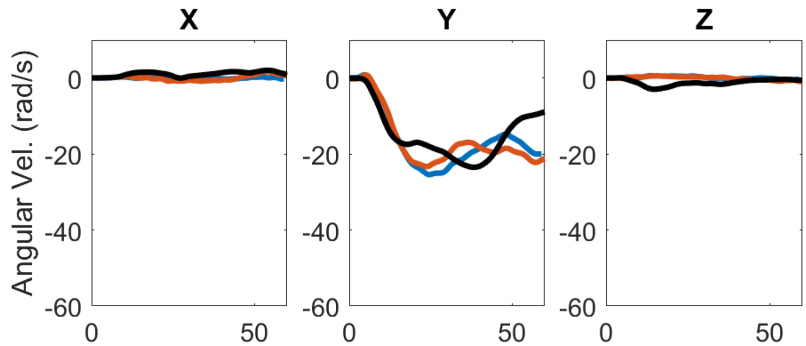

5.5 m/s

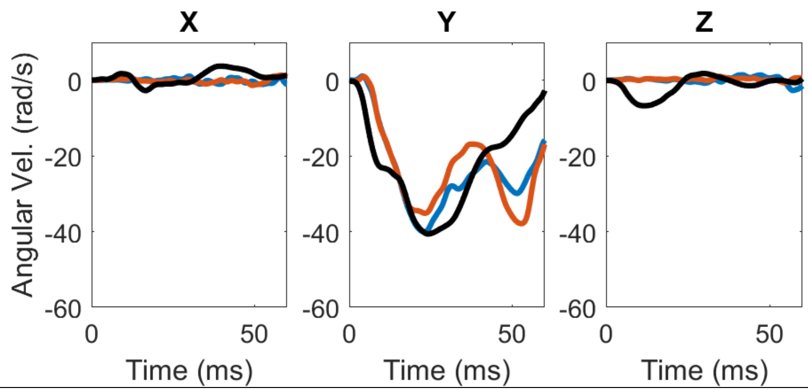

9.3 m/s

Rear Orientation

Figure S3 Head Angular Velocity (3DOF) in all impacts

Supplemental Materials D: Head Angular Acceleration (3DOF) in all impacts

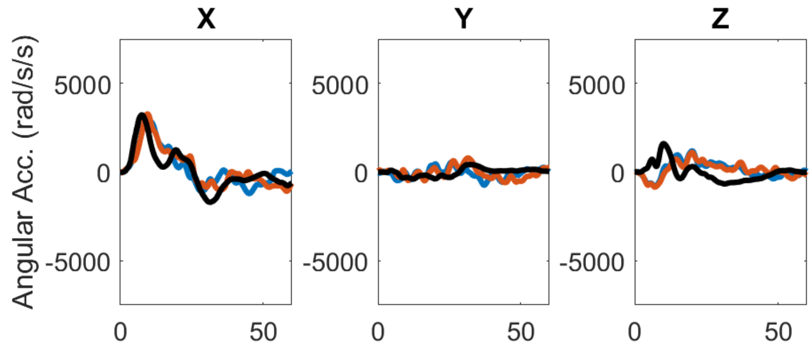

5.5 m/s

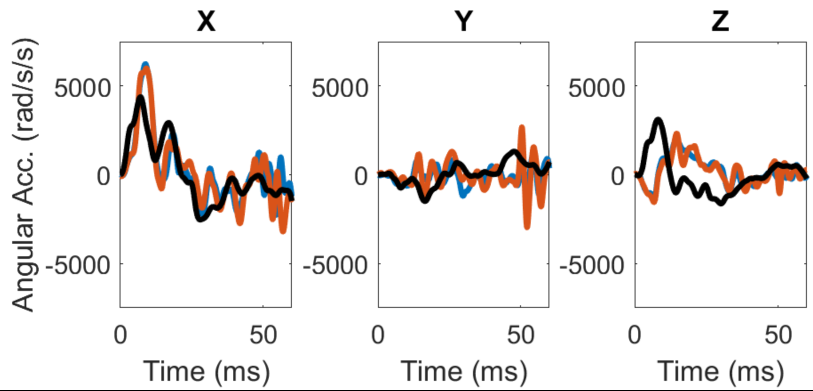

9.3 m/s

Lateral Orientation

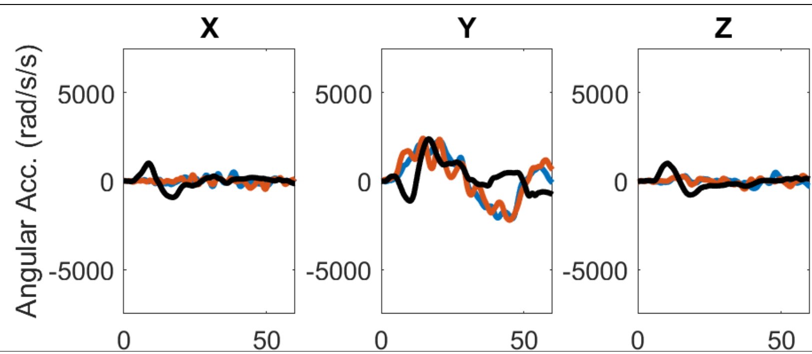

5.5 m/s

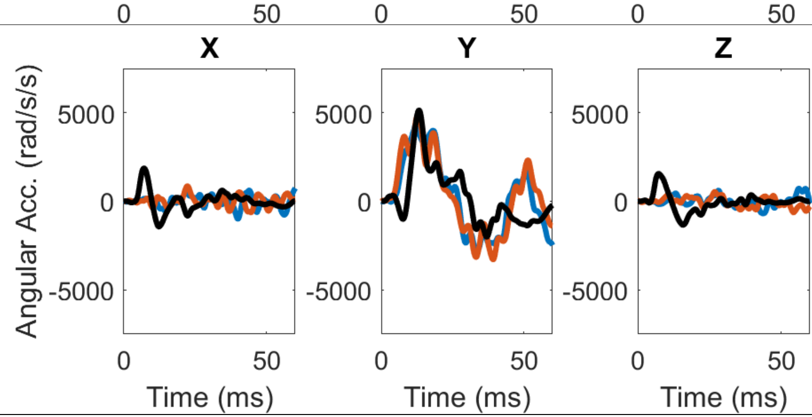

9.3 m/s

Frontal Orientation

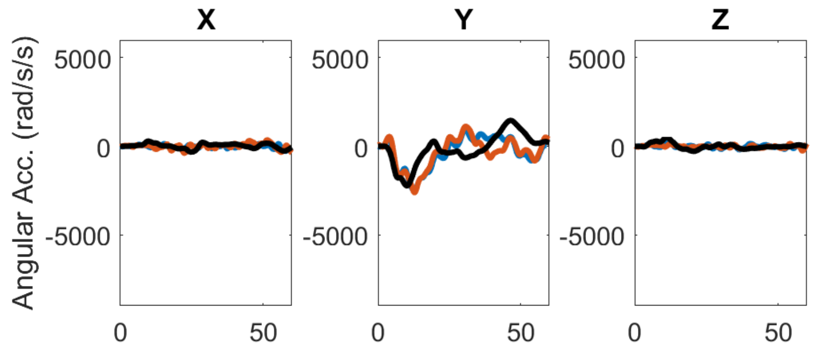	5.5 m/s
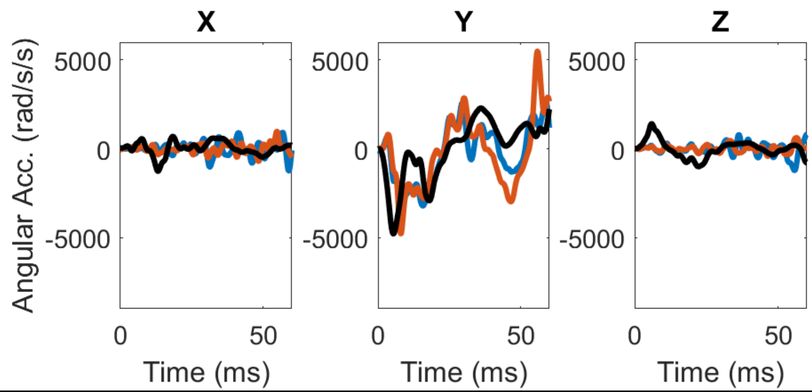	9.3 m/s
Rear Orientation	

Figure S4 Head Angular Acceleration (3DOF) in all impacts

Supplemental Materials E: Head Linear Velocity (3DOF) in all impacts

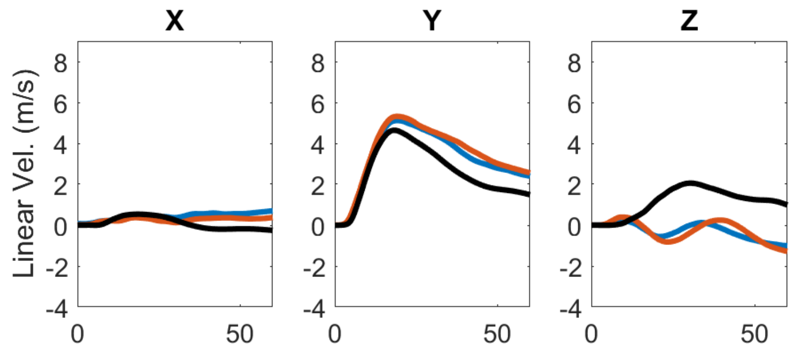

5.5 m/s

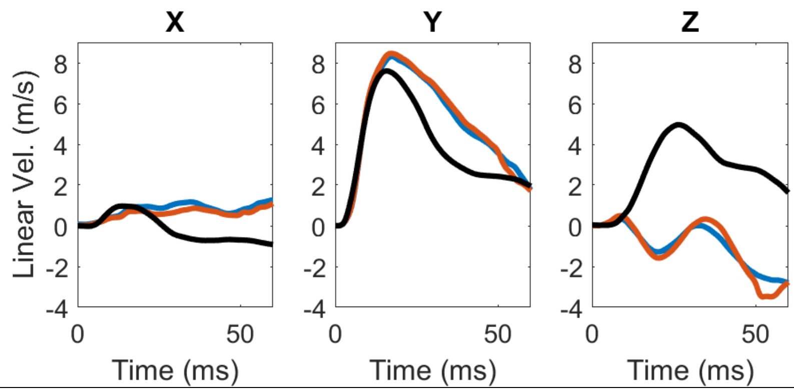

9.3 m/s

Lateral Orientation

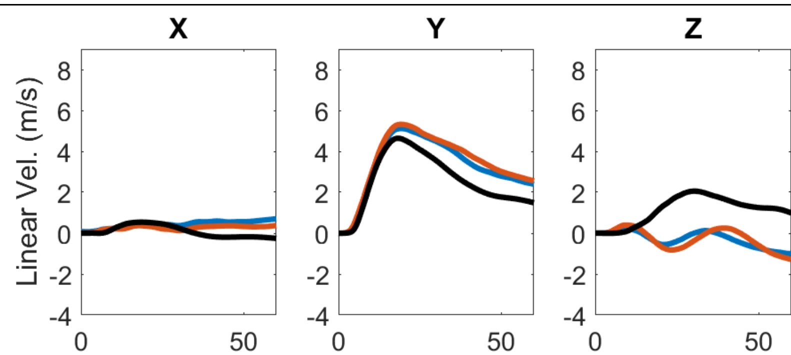

5.5 m/s

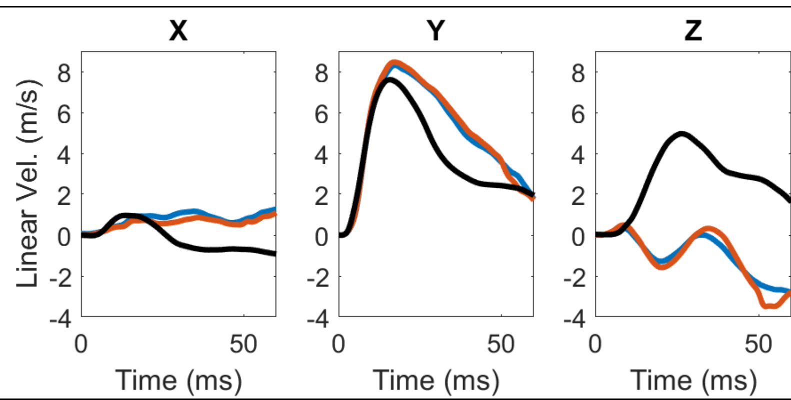

9.3 m/s

Frontal Orientation

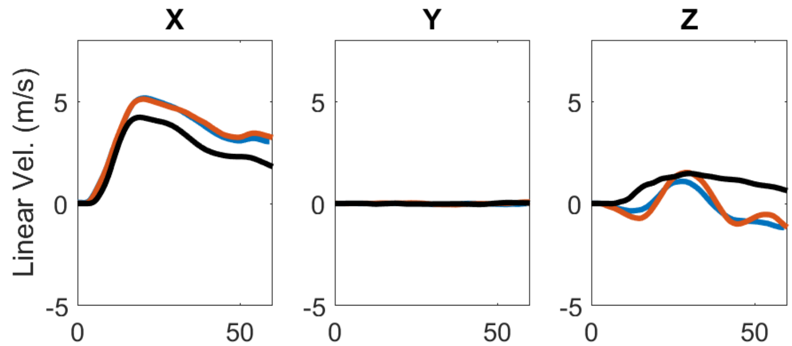

5.5 m/s

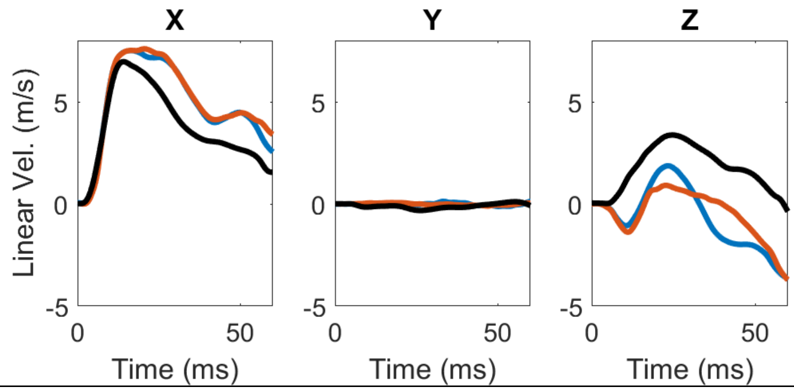

9.3 m/s

Rear Orientation

Figure S5 Head Linear Velocity (3DOF) in all impacts

Supplemental Materials F: Head Linear Acceleration (3DOF) in all impacts

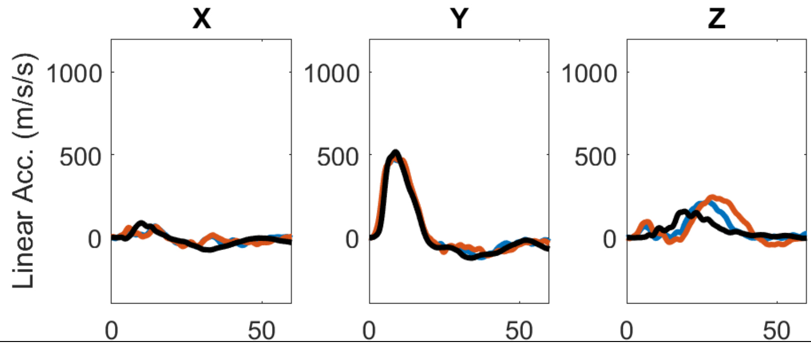

5.5 m/s

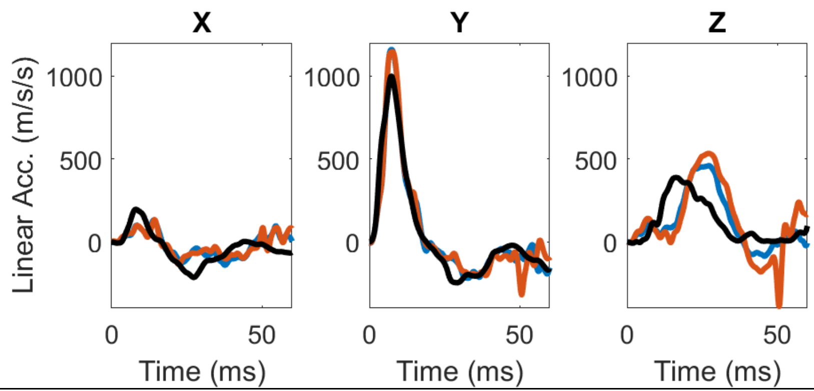

9.3 m/s

Lateral Orientation

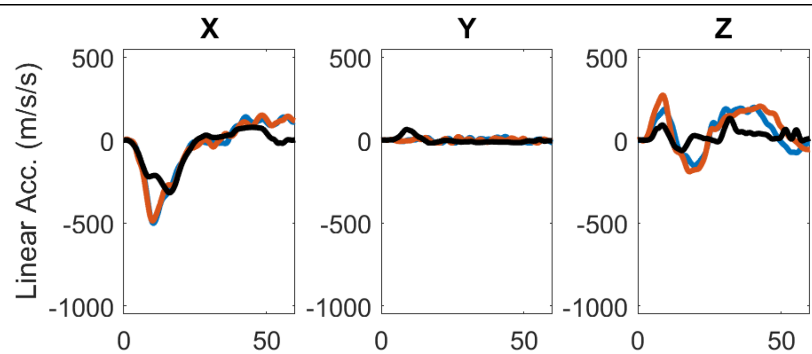

5.5 m/s

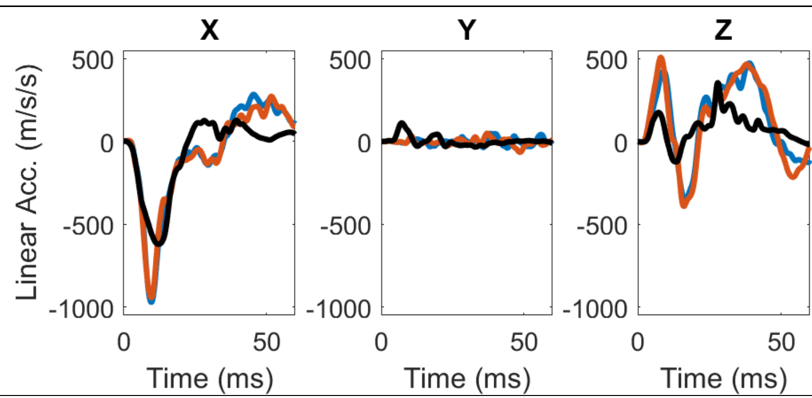

9.3 m/s

Frontal Orientation

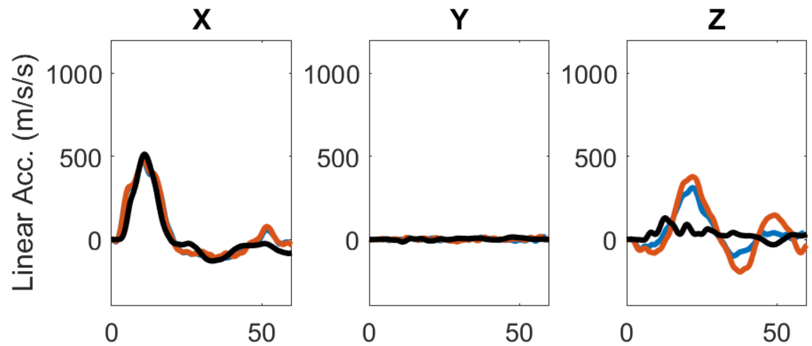	5.5 m/s
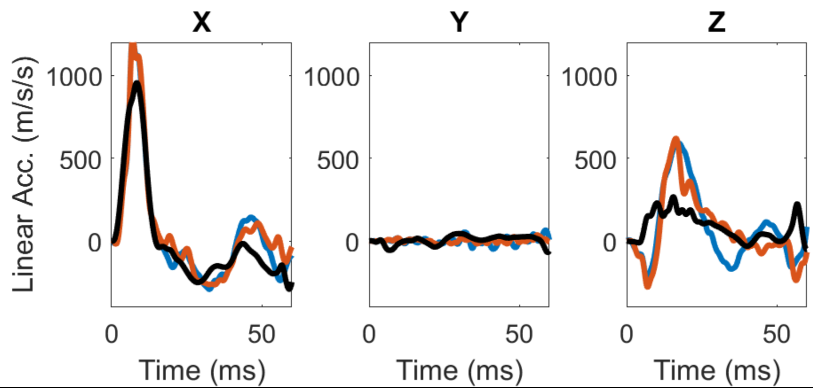	9.3 m/s
Rear Orientation	

Figure S6 Head Linear Acceleration (3DOF) in all impacts